Comput Econ (2012) 40:63–104
DOI 10.1007/s10614-011-9269-8

Using Pseudo-Parabolic and Fractional Equations for Option Pricing in Jump Diffusion Models

Andrey Itkin · Peter Carr

Accepted: 30 May 2011 / Published online: 21 June 2011

Abstract In mathematical finance a popular approach for pricing options under some Lévy model would be to consider underlying that follows a Poisson jump diffusion process. As it is well known this results in a partial integro-differential equation (PIDE) that usually does not allow an analytical solution, while a numerical solution also faces some problems. In this paper we develop a new approach on how to transform the PIDE into a class of so-called pseudo-parabolic equations which are well known in mathematical physics but are relatively new for mathematical finance. As an example we will discuss several jump-diffusion models which Lévy measure allows such a transformation.

Keywords Pseudo-parabolic equations · Jump-diffusion · Finite-difference scheme · Numerical method · The Green function · General stable tempered process

Mathematics Subject Classification (2000) 60J75 · 35M99 · 65L12 · 65L20 · 34B27 · 65T50

1 Introduction

In mathematical finance a popular approach for pricing options under some Lévy model would be to consider underlying that follows a Poisson jump diffusion process.

A. Itkin (✉)
New York University Polytechnic Institute, 6 Metro Tech Center, RH 517E, Brooklyn, NY 11201, USA
e-mail: aitkin@poly.edu

P. Carr
Morgan Stanley, 585 Broadway, New York, NY 10036, USA
e-mail: Peter.P.Carr@morganstanley.com

P. Carr
New York University, New York, NY, USA

As it is well known this results in a partial integro-differential equation (PIDE) that usually does not allow an analytical solution while a numerical solution also faces some problems. These problems are mainly related to computation of a non-local integral term, whereas computation of a differential part of the PIDE, discussed numerous times in the literature, can be provided in a relatively standard way. Furthermore, it is always possible to reduce the whole PIDE to a set of the simpler equations using a splitting technique. This set, in fact, will contain just pure one-dimensional unsteady PDE and pure evolutionary-integral equations (EIDE) (see, for instance, In't Hout and Welfert 2009; Itkin and Carr 2006). Here we are not concerned with the solutions of the former equations. However, we do consider how to efficiently solve the latter equations that is the main subject of this paper.

A thorough description of methods used for solving this kind of equations is given in Cont (2009) and Hilber et al. (2009). Some problems related to implementation of these methods are also discussed in Carr and Mayo (2007) and Strauss (2006).

According to the last cited publication we could distinguish the following methods that are currently used to solve the EIDE. In an early paper, Amin (1993) used an explicit multinomial tree based approach. d'Halluin et al. (2004, 2005) implemented implicit methods for evaluating vanilla European options, barrier options, and American options. They also showed that when a log spaced grid is used with a Crank Nicolson discretization on a problem with constant parameters the resulting scheme is unconditionally strictly stable. In addition, they showed that the simple Picard iteration scheme (also suggested in Tavella and Randall 2000) for solving the discretized equations is globally convergent. Specifically, they reported that when they priced options in the Merton model the error was reduced by two orders of magnitude at each iteration for typical values of the time step size and Poisson arrival intensity. More recently, d'Halluin et al. (2005) presented a semi-Lagrangian approach for pricing American Asian options under jump diffusion processes. Andersen and Andreasen (2000) derived a forward equation describing the evolution of European call options as functions of strike and maturity, and discussed its application to the problem of fitting the stock process to option prices in the market. They also presented a second order accurate unconditionally stable operator splitting (ADI) method for pricing options which does not require iterative solution of an algebraic equation at each time step. (Unfortunately, it is not clear how to extend their method to the valuation of American options while retaining second order accuracy.) Cont and Voltchkova (2003) used a discretization that is implicit in the differential terms and implicit in the integral term, and showed that it converges to a viscosity solution. Their method extends to infinite activity models, and does not require the diffusion part of the equation to be non-degenerate. These PIDEs have also been solved by many others. See, for example, Zhang (1993) and Matache et al. (2002). Although the pricing equations have often been solved numerically, because of the integrals in the equations the methods have proven to be relatively expensive. The obvious discretizations of the pricing equations combine standard discretization methods for the differential terms with quadrature methods such as Simpson's rule or Gaussian quadrature for evaluating the integral term. This approach is computationally expensive since the integral must be approximated at each point of the mesh used for discretizing the differential terms. The difficulties are greater if an implicit discretization of both the integral and the differential terms is used.

The expense of evaluating the integral at all points of the computational grid can, however, be reduced by making the same exponential change of variables often used when solving the Black–Scholes differential equation with no jumps. This converts the integral term into a correlation integral which can be evaluated at all the mesh points simultaneously using the Fast Fourier Transform. This approach has been suggested by many authors (Wilmott 1998; Tavella and Randall 2000; Andersen and Andreasen 2000).

Various kind of finite elements methods were proposed for multidimensional Lévy processes (see survey in Hilber et al. 2009) since finite difference methods are not efficient when dimensionality of the problem exceeds the number of 3.

Also worth noting a new method for exponential jumps proposed by Lipton and Sepp (2009) who calculate the jump integral recursively on the spatial grid. This is a special trick for exponential jumps and it does not work for more familiar Gaussian jumps. The authors claim that a simple interpolation routine is sufficient for discrete jumps.

As Carr and Mayo mentioned (see Carr and Mayo 2007) quadrature methods are expensive since the integrals must be evaluated at every point of the mesh. Though less so, Fourier methods are also computationally intensive since in order to avoid wrap around effects they require enlargement of the computational domain. They are also slow to converge when the parameters of the jump process are not smooth, and require uniform meshes for efficiency. Therefore, they proposed a different and more efficient class of methods which are based on the fact that the integrals often satisfy differential equations. Depending on the process the asset follows, the equations are either ordinary differential equations or parabolic partial differential equations. Both types of equations can be accurately solved very rapidly. Carr and Mayo (2007) used to demonstrate the advantage of such an approach for the Merton and Kou models. However, the extension of their idea for other types of the Lévy models is yet unknown.

Therefore in this paper we propose two different approaches. The idea of the first one is to represent a Lévy measure as the Green's function of some yet unknown differential operator $\mathcal{A}$. If we manage to find an explicit form of this operator then the original PIDE will reduce to a new type of equation—a so-called pseudo-parabolic equation. These equations are known in mathematical physics (see, for instance, Cannon and Lin 1988) but are new in mathematical finance.

Then we rely on two important results, namely: (a) the inverse operator $\mathcal{A}^{-1}$ exists, and (b) the obtained pseudo parabolic equation could be formally solved analytically via a matrix exponent. Having that we discuss a numerical method of how to compute this matrix exponent. We show that this can be done using a finite difference scheme similar to that used for solving the parabolic PDEs, and the matrix of this finite-difference method (FD) scheme is banded. We fulfill this program for general tempered stable processes (GTSP)[1] with an integer damping exponent α.

Alternatively for the same class of the Lévy processes (GTSP/KoBoL/SSM) with the real dumping exponent α we show how to transform the corresponding PIDE to a fractional PDE (method 2). Fractional PDEs for the Lévy processes with finite variation were derived by Boyarchenko and Levendorskii (2002) and later by

[1] In the literature they are also known as KoBol or SSM processes.

Cartea and del Castillo-Negrete (2007) using a characteristic function technique. Numerical solution of these equations was investigated by Cartea and del Castillo-Negrete (2007) and Marom and Momoniat (2009). In this paper we derive them in all cases, including processes with infinite variation, using a different technique—shift operators. Then to solve them we apply a new method, namely: having results computed for $\alpha \in \mathbb{Z}$ we then interpolate them with the second order in α to obtain the solution at any $\alpha \in \mathbb{R}$.

We also show that despite a common practice to integrate out all Lévy compensators in the integral term when considered jumps are of finite activity and finite variation, this, in fact, breaks the stability of the scheme, at least for the fractional PDE. Therefore, in order to construct the unconditionally stable scheme one must keep the other terms under the integrals. To resolve this, Cartea and del Castillo-Negrete (2007) were compelled to change their definition of the fractional derivative.

It is important to note that the proposed methods could be easily generalized for the time-dependent Lévy density.

The rest of the paper is organized as follows. In Sect. 2 we discuss a basic example of the method provided that the simple exponential Lévy measure is used to describe the jumps. In the next section we consider GTSP models and show how to reduce the corresponding PIDE to the pseudo parabolic equation in this case. Section 4 describes the numerical solution of the obtained pseudo parabolic equations in case $\alpha \in \mathbb{Z}$. Section 5 focuses on the general case of real α and introduces our method of deriving fractional PDE based on the shift operators. In Sect. 6 we discuss how to solve these FPDE by constructing unconditionally stable finite difference schemes of high order of accuracy in space and time, and provide some numerical examples and comparison with the other methods. The last section concludes.

2 Basic Example

In this section we examine the simplest possible problem to demonstrate the basics of our new method. We assume no arbitrage so that there exists a risk-neutral measure $\mathbb{Q}$. We assume zero interest rates and dividends so that the stock price is a $\mathbb{Q}$-martingale. Suppose that the underlying stock price process is pure jump (i.e. there is no continuous martingale component). Further suppose that the jump process is a compound Poisson process. The arrival rate of a jump is constant at $\lambda > 0$, while the jump size distribution is a symmetric Laplace distribution, i.e the probability density for a jump of size $j \in \mathbb{R}$, given that a jump has occurred is given by:

$$q(j) = \frac{\alpha e^{-\alpha|j|}}{2}, \quad j \in \mathbb{R}, \tag{1}$$

where $\alpha > 0$ is a free parameter. We recognize that these dynamics let prices become negative and ignore this complication. Let $u(x, t)$ be the value of the contingent claim at calendar time $t \in [0, T]$ given that the time t stock price is $x \in \mathbb{R}$. As a result of our assumptions, the contingent claim value solves the following PIDE:

$$\frac{\partial}{\partial t}u(x,t) + \lambda \int_{\mathbb{R}} [u(x+j,t) - u(x,t) - \frac{\partial}{\partial x}u(x,t)j]q(j)dj = 0, \tag{2}$$

on the domain $x \in \mathbb{R}$, $t \in [0, T]$. For a European call, the terminal condition is

$$u(x,T) = (x-K)^+, \quad x \in \mathbb{R}, \tag{3}$$

where $K \in \mathbb{R}$ is the strike price.

Now the symmetry of the PDF in (1) implies that:

$$\int_{\mathbb{R}} jq(j)dj = 0, \tag{4}$$

and hence the PIDE (2) simplifies to:

$$\frac{\partial}{\partial t}u(x,t) - \lambda u(x,t) + \lambda \int_{\mathbb{R}} u(x+j,t)q(j)dj = 0. \tag{5}$$

If we do the change of variable $z = -j$ in the integral, we obtain a convolution:

$$\frac{\partial}{\partial t}u(x,t) - \lambda u(x,t) + \lambda \int_{\mathbb{R}} u(x-z,t)q(z)dz = 0. \tag{6}$$

If we do the change of variable $y = x - z$ in the integral, we obtain:

$$\frac{\partial}{\partial t}u(x,t) - \lambda u(x,t) + \lambda \int_{\mathbb{R}} u(y,t)q(x-y)dy = 0. \tag{7}$$

Now consider the simple second order linear inhomogeneous ODE:

$$g''(x) - \alpha^2 g(x) = -\delta(x), \quad x \in \mathbb{R}, \tag{8}$$

where $\delta(x)$ denotes Dirac's delta function. Suppose that the ODE is to be solved subject to the boundary conditions:

$$\lim_{x \to \pm\infty} g(x) = 0. \tag{9}$$

The solution to this problem is usually referred to as a Green's function. The solution is well known to be:

$$g(x) = \frac{e^{-\alpha|x|}}{2\alpha}. \tag{10}$$

Comparing (10) and (1), we see that:

$$q(x) = \alpha^2 g(x). \tag{11}$$

Hence, the PIDE (16) can be re-written as:

$$\frac{\partial}{\partial t}u(x,t) - \lambda u(x,t) + \lambda\alpha^2 \int\limits_{\mathbb{R}} u(y,t)g(x-y)dy = 0. \tag{12}$$

To exploit the connection (11), let $\mathcal{D}_x$ denote the first derivative operator and let $\mathcal{A}_x$ denote the following linear differential operator:

$$\mathcal{A}_x \equiv \mathcal{D}_x^2 - \alpha^2 \mathcal{I}_x, \tag{13}$$

where $\mathcal{I}_x$ is the identity operator.

Using this operator notation, the ODE (8) reads:

$$\mathcal{A}_x g(x) = -\delta(x). \tag{14}$$

Suppose that we apply the $\mathcal{A}_x$ operator to (12):

$$\mathcal{A}_x \frac{\partial}{\partial t}u(x,t) - \lambda \mathcal{A}_x u(x,t) + \lambda\alpha^2 \int\limits_{\mathbb{R}} u(y,t)\mathcal{A}_x g(x-y)dy = 0. \tag{15}$$

where we have assumed that the interchange of the integral and the differential operator is permissible. Substituting (14) in (12) implies that:

$$\mathcal{A}_x \frac{\partial}{\partial t}u(x,t) - \lambda \mathcal{A}_x u(x,t) - \lambda\alpha^2 \int\limits_{\mathbb{R}} u(y,t)\delta(x-y)dy = 0. \tag{16}$$

Using the sifting property of the delta function implies that our problem reduces to a (third order) PDE:

$$\mathcal{A}_x \frac{\partial}{\partial t}u(x,t) - \lambda \mathcal{A}_x u(x,t) - \lambda\alpha^2 u(x,t) = 0. \tag{17}$$

Substituting (13) in (17) and simplifying implies:

$$\frac{\partial^3}{\partial x^2 \partial t}u(x,t) - \alpha^2 \frac{\partial}{\partial t}u(x,t) - \lambda \frac{\partial^2}{\partial x^2}u(x,t) = 0. \tag{18}$$

Thus, we managed to transform the original PIDE to the PDE which, however, is of a new type. This is not a pure parabolic equation because it contains mixed derivatives in time and space. Fortunately, such equations are well known in physics and called

"pseudo-parabolic". We will show later that the solution of these equations could be obtained by using standard finite-difference methods.

Note that a similar transformation could be derived for some other types of the jump size distribution. For instance, for Erlang distributions (Evans et al. 2000), which are the generalization of the exponential type kernels, we can proceed in the same manner, but by replacing the second order differential operator $\mathcal{A}_x$ with a higher order differential operator. We also know from Carr and Mayo (2007) that transformation from PIDE to PDE is possible for the Gaussian type jumps. Having that in the rest of the paper we want to demonstrate how to accomplish the same program for a more complicated type of jumps which follow Generalized Tempered Stable Processes (GTSP).

3 GTSP/KoBoL/SSM Model

Stochastic skew model (SSM) has been proposed by Carr and Wu (2004) for pricing currency options. It makes use of a Lévy model also known as generalized tempered stable processes (see Cont and Tankov 2004) for the dynamics of stock prices which generalize the CGMY processes proposed by Carr et al. (2002). A similar model was independently proposed by Koponen (1995) and then Boyarchenko and Levendorskii (2002) The processes are obtained by specifying a more generalized Lévy measure with two additional parameters. These two parameters provide control on asymmetry of small jumps and different frequencies for upward and downward jumps. The results of Zhou (2006) show that this generalization allows for more accurate pricing of options.

GTSP have probability densities symmetric in a neighborhood of the origin and exponentially decaying in the far tails. After this exponential softening, the small jumps keep their initial stable-like behavior, whereas the large jumps become exponentially tempered. The Lévy measure of GTSP reads

$$\mu(y) = \lambda_- \frac{e^{-\nu_-|y|}}{|y|^{1+\alpha_-}} \mathbf{1}_{y<0} + \lambda_+ \frac{e^{-\nu_+|y|}}{|y|^{1+\alpha_+}} \mathbf{1}_{y>0}, \tag{19}$$

where $\nu_\pm > 0$, $\lambda_\pm > 0$ and $\alpha_\pm < 2$. The last condition is necessary to provide

$$\int_{-1}^{1} y^2 \mu(dy) < \infty, \quad \int_{|y|>1} \mu(dy) < \infty. \tag{20}$$

The case $\lambda_+ = \lambda_-, \alpha_+ = \alpha_-$ corresponds to the CGMY process. The limiting case $\alpha_+ = \alpha_- = 0, \lambda_+ = \lambda_-$ is the special case of the Variance Gamma process of Madan and Seneta (1990). As mentioned in (Zhou 2006) six parameters of the model play an important role in capturing various aspects of the stochastic process. The parameters $\lambda_\pm$ determine the overall and relative frequencies of upward and downward jumps. If we are interested only in jumps larger than a given value, these two parameters tell us how often we should expect such events. $\nu_\pm$ control the tail behavior of the Lévy measure, and they tell us how far the process may jump. They also lead to skewed

distributions when they are unequal. In the special case when they are equal, the Lévy measure is symmetric. Finally, $\alpha_\pm$ are particularly useful for the local behavior of the process. They determine whether the process has finite or infinite activity, or variation.

Using this model of jumps Carr and Wu (2004) derived the following PIDE which governs an arbitrage-free value of a European call option at time t

$$
\begin{aligned}
&r_d C(S,V_R,V_L,t)\\
&\quad=\frac{\partial}{\partial t}C(S,V_R,V_L,t)+(r_d-r_f)S\frac{\partial}{\partial S}C(S,V_R,V_L,t)\\
&\quad+\kappa(1-V_R)\frac{\partial}{\partial V_R}C(S,V_R,V_L,t)+\kappa(1-V_L)\frac{\partial}{\partial V_L}C(S,V_R,V_L,t)\\
&\quad+\frac{\sigma^2S^2(V_R+V_L)}{2}\frac{\partial^2}{\partial S^2}C(S,V_R,V_L,t)+\sigma\rho^R\sigma_V SV_R\frac{\partial^2}{\partial S\partial V_R}C(S,V_R,V_L,t)\\
&\quad+\sigma\rho^L\sigma_V SV_L\frac{\partial^2}{\partial S\partial V_L}C(S,V_R,V_L,t)+\frac{\sigma_V^2V_R}{2}\frac{\partial^2}{\partial V_R^2}C(S,V_R,V_L,t)\\
&\quad+\frac{\sigma_V^2V_L}{2}\frac{\partial^2}{\partial V_L^2}C(S,V_R,V_L,t)\\
&\quad+\sqrt{V_R}\int_0^\infty\left[C(Se^y,V_R,V_L,t)-C(S,V_R,V_L,t)-\frac{\partial}{\partial S}C(S,V_R,V_L,t)S(e^y-1)\right]\\
&\quad\times\lambda\frac{e^{-\nu_R|y|}}{|y|^{1+\alpha}}dy\\
&\quad+\sqrt{V_L}\int_{-\infty}^0\left[C(Se^y,V_R,V_L,t)-C(S,V_R,V_L,t)-\frac{\partial}{\partial S}C(S,V_R,V_L,t)S(e^y-1)\right]\\
&\quad\times\lambda\frac{e^{-\nu_L|y|}}{|y|^{1+\alpha}}dy,
\end{aligned}
\tag{21}
$$

on the domain $S>0, V_R>0, V_L>0$ and $t\in[0,T]$, where S, V_R, V_L are state variables (spot price and stochastic variances). For the following some important observations have to be made.

1. This PIDE could be generalized with allowance for GTSP processes, which means we substitute α in Eq. 21 with α_R, α_L, and λ with λ_R, λ_L correspondingly.
2. The obtained PIDE could be solved by using a splitting technique (see Itkin and Carr 2006). In more detail the numerical solution of the PIDE could be found in several steps. At every step we have to solve a certain simpler subproblem. These subproblems include either solution of one-dimensional advection-diffusion PDE with no jumps, or solution of a pure evolutionary jump equation (with no diffusion and drift terms) of the type equation (2).
3. To demonstrate the idea of our method we start by considering the jumps with only the finite activity, i.e. $\alpha_R<0, \alpha_L<0$. Therefore, each compensator under the

integral could be integrated out. In the next sections a general case $\alpha_R < 2, \alpha_L < 2$ will be discussed as well.

We assume that the advection-diffusion equations can be solved by using a standard finite-difference technique, hence this is not a subject of our paper. We do consider only those steps of the splitting method which deal with the remaining integral term. The corresponding equation reads

$$\frac{\partial}{\partial t}C(S, V_R, V_L, t) = -\sqrt{V_R}\int_0^\infty C(Se^y, V_R, V_L, t)\lambda_R \frac{e^{-\nu_R|y|}}{|y|^{1+\alpha_R}}dy \tag{22}$$

for positive jumps and

$$\frac{\partial}{\partial t}C(S, V_R, V_L, t) = -\sqrt{V_L}\int_{-\infty}^0 C(Se^y, V_R, V_L, t)\lambda_L \frac{e^{-\nu_L|y|}}{|y|^{1+\alpha_L}}dy \tag{23}$$

for negative jumps.

Making a change of variables $x = \log S$ and omitting dependence on dummy variables V_R, V_L we can rewrite these two equations in a more standard form

$$\begin{aligned}\frac{\partial}{\partial t}C(x, t) &= -\sqrt{V_R}\int_0^\infty C(x + y, t)\lambda_R \frac{e^{-\nu_R|y|}}{|y|^{1+\alpha_R}}dy \\ \frac{\partial}{\partial t}C(x, t) &= -\sqrt{V_L}\int_{-\infty}^0 C(x + y, t)\lambda_L \frac{e^{-\nu_L|y|}}{|y|^{1+\alpha_L}}dy\end{aligned} \tag{24}$$

To make it clear the above is not a system of equations but rather two different steps of the splitting procedure.

In the first integral y varies in $[0, \infty]$, and in the second one—in $[-\infty, 0]$, while the kernel of both integrals vanishes at $y = 0$. Therefore, nothing changes if we rewrite the above equations in the form

$$\begin{aligned}\frac{\partial}{\partial t}C(x, t) &= -\sqrt{V_R}\int_0^\infty C(x + y, t)\lambda_R \frac{e^{-\nu_R|y|}}{|y|^{1+\alpha_R}}\mathbf{1}_{y>0}dy \\ \frac{\partial}{\partial t}C(S, t) &= -\sqrt{V_L}\int_{-\infty}^0 C(x + y, t)\lambda_L \frac{e^{-\nu_L|y|}}{|y|^{1+\alpha_L}}\mathbf{1}_{y<0}dy\end{aligned} \tag{25}$$

This two equations are still PIDE or evolutionary integral equations. We want to apply our new method to transform them to a certain pseudo parabolic equations.

First equation in Eq. 25 Assuming $z = x + y$ we rewrite it in the form

$$\frac{\partial}{\partial t}C(x,t) = -\sqrt{V_R}\int\limits_{x}^{\infty} C(z,t)\lambda_R \frac{e^{-\nu_R|z-x|}}{|z-x|^{1+\alpha_R}}\mathbf{1}_{z-x>0}dz \tag{26}$$

To achieve our goal we have to solve the following problem. We need to find a differential operator $\mathcal{A}_y^+$ which Green's function is the kernel of the integral in Eq. 26, i.e.

$$\mathcal{A}_y^+\left[\lambda\frac{e^{-\nu|y|}}{|y|^{1+\alpha}}\mathbf{1}_{y>0}\right] = \delta(y) \tag{27}$$

We prove the following proposition.

Proposition 1 *Assume that in Eq. 27 $\alpha \in \mathbb{Z}$, and $\alpha < 0$. Then the solution of Eq. 27 with respect to $\mathcal{A}_y^+$ is*

$$\mathcal{A}_y^+ = \frac{1}{\lambda p!}\left(\nu + \frac{\partial}{\partial y}\right)^{p+1} \equiv \frac{1}{\lambda p!}\left[\sum_{i=0}^{p+1} C_i^{p+1}\nu^{p+1-i}\frac{\partial^i}{\partial y^i}\right], \quad p \equiv -(1+\alpha) \geq 0,$$

where C_i^{p+1} are the binomial coefficients.

Proof This result could be proven by taking Laplace transform of both parts of Eq. 27 (see below). It could be also verified using any symbolic processor, e.g. Mathematica. □

Second equation in Eq. 25 For the second equation in Eq. 25 it is possible to elaborate an analogous approach. Again assuming $z = x + y$ we rewrite it in the form

$$\frac{\partial}{\partial t}C(x,t) = -\sqrt{V_L}\int\limits_{-\infty}^{x} C(z,t)\lambda_R \frac{e^{-\nu_R|z-x|}}{|z-x|^{1+\alpha_R}}\mathbf{1}_{z-x<0}dz \tag{28}$$

Now we need to find a differential operator $\mathcal{A}_y^-$ which Green's function is the kernel of the integral in Eq. 28, i.e.

$$\mathcal{A}_y^-\left[\lambda\frac{e^{-\nu|y|}}{|y|^{1+\alpha}}\mathbf{1}_{y<0}\right] = \delta(y) \tag{29}$$

We prove the following proposition.

Proposition 2 *Assume that in Eq. 29 $\alpha \in \mathbb{Z}$, and $\alpha < 0$. Then the solution of Eq. 29 with respect to $\mathcal{A}_y^-$ is*

$$\mathcal{A}_y^- = \frac{1}{\lambda p!}\left(\nu - \frac{\partial}{\partial y}\right)^{p+1} \equiv \frac{1}{\lambda p!}\left[\sum_{i=0}^{p+1}(-1)^i C_i^{p+1}\nu^{p+1-i}\frac{\partial^i}{\partial y^i}\right], \quad p \equiv -(1+\alpha),$$

Proof Using Laplace transform one can check the above result for any positive integer p. □

To proceed we need to prove two other statements.

Proposition 3 *Let us denote the kernels as*

$$g^+(z-x) \equiv \lambda_R \frac{e^{-\nu_R|z-x|}}{|z-x|^{1+\alpha_R}} \mathbf{1}_{z-x>0}. \tag{30}$$

Then

$$\mathcal{A}_x^- g^+(z-x) = \delta(z-x). \tag{31}$$

Proof

$$\begin{aligned}\mathcal{A}_x^- g^+(z-x) &= \frac{1}{\lambda p!}\left(\nu - \frac{\partial}{\partial x}\right)^{p+1} g^+(z-x) \\ &= \frac{1}{\lambda p!}\left(\nu + \frac{\partial}{\partial (z-x)}\right)^{p+1} g^+(z-x) = \mathcal{A}_{z-x}^+ g^+(z-x) = \delta(z-x)\end{aligned}$$

□

Proposition 4 *Let us denote the kernels as*

$$g^-(z-x) \equiv \lambda_L \frac{e^{-\nu_L|z-x|}}{|z-x|^{1+\alpha_L}} \mathbf{1}_{z-x<0}. \tag{32}$$

Then

$$\mathcal{A}_x^+ g^-(z-x) = \delta(z-x). \tag{33}$$

Proof

$$\begin{aligned}\mathcal{A}_x^+ g^-(z-x) &= \frac{1}{\lambda p!}\left(\nu + \frac{\partial}{\partial x}\right)^{p+1} g^-(z-x) \\ &= \frac{1}{\lambda p!}\left(\nu - \frac{\partial}{\partial (z-x)}\right)^{p+1} g^-(z-x) \\ &= \mathcal{A}_{z-x}^- g^-(z-x) = \delta(z-x)\end{aligned}$$

□

Transformation We now apply the operator $\mathcal{A}_x^-$ to both parts of Eq. 26 to obtain

$$\begin{aligned}\mathcal{A}_x^- \frac{\partial}{\partial t} C(x,t) &= -\sqrt{V_R}\mathcal{A}_x^- \int_x^\infty C(z,t) g^+(z-x)dz \\ &= -\sqrt{V_R}\left\{\int_x^\infty C(z,t)\mathcal{A}_x^- g^+(z-x)dz + \mathcal{R}\right\} \\ &= -\sqrt{V_R}\left\{\int_x^\infty C(z,t)\delta(z-x)dz + \mathcal{R}\right\} = -\frac{1}{2}\sqrt{V_R}C(x,t) - \sqrt{V_R}\mathcal{R}\end{aligned} \tag{34}$$

Here

$$\mathcal{R} = \sum_{i=0}^{p} a_i \left(\frac{\partial^{p-i}}{\partial x^{p-i}} V(x)\right)\left(\frac{\partial^i}{\partial x^i} g(z-x)\right)\Big|_{z-x=0}, \tag{35}$$

and a_i are some constant coefficients. As from the definition in Eq. 30 $g(z-x) \propto (z-x)^p$, the only term in Eq. 35 which does not vanish is that at $i = p$. Thus

$$\mathcal{R} = V(x)\left(\frac{\partial^p}{\partial x^p} g(z-x)\right)\Big|_{z-x=0} = V(x)p!\mathbf{1}_{(0)} = 0; \tag{36}$$

With allowance for this expression from Eq. 34 we obtain the following pseudo parabolic equation for $C(x,t)$

$$\mathcal{A}_x^- \frac{\partial}{\partial t} C(x,t) = -\frac{1}{2}\sqrt{V_R}C(x,t) \tag{37}$$

Applying the operator $\mathcal{A}_x^+$ to both parts of the second equation in Eq. 28 and doing in the same way as in the previous paragraph we obtain the following pseudo parabolic equation for $C(x,t)$

$$\mathcal{A}_x^+ \frac{\partial}{\partial t} C(x,t) = -\frac{1}{2}\sqrt{V_L}C(x,t) \tag{38}$$

4 Solution of the Pseudo Parabolic Equation

Assume that the inverse operator $\mathcal{A}^{-1}$ exists (see discussion later) we can represent, for instance, Eq. 37 in the form

$$\frac{\partial}{\partial t} C(x,t) = -\mathcal{B}C(x,t), \quad \mathcal{B} \equiv \frac{1}{2}\sqrt{V_R}(\mathcal{A}_x^-)^{-1}, \tag{39}$$

This equation can be formally solved analytically to give

$$C(x,t) = e^{\mathcal{B}(T-t)}C(x,T), \tag{40}$$

where T is the time to maturity and $C(x,T)$ is payoff. Switching to a new variable $\tau = T - t$ to go backward in time we rewrite Eq. 40 as

$$C(x,\tau) = e^{\mathcal{B}\tau}C(x,0), \tag{41}$$

Below we consider numerical methods which allow one to compute this operator exponent with a prescribed accuracy. First we consider a straightforward approach when $\alpha \in \mathbb{Z}$.

4.1 Numerical Method when $\alpha \in \mathbb{Z}$

Suppose that the whole time space is uniformly divided into N steps, so the time step $\theta = T/N$ is known. Assuming that the solution at time step k, $0 \le k < N$ is known and we go backward in time, we could rewrite Eq. 40 in the form

$$C^{k+1}(x) = e^{\mathcal{B}\theta}C^k(x), \tag{42}$$

where $C^k(x) \equiv C(x,k\theta)$. To get representation of the rhs of Eq. 42 with given order of approximation in θ, we can substitute the whole exponential operator with its Padé approximation of the corresponding order m.

First, consider the case $m = 1$. A symmetric Padé approximation of the order $(1,1)$ for the exponential operator is

$$e^{\mathcal{B}\theta} = \frac{1 + \mathcal{B}\theta/2}{1 - \mathcal{B}\theta/2} \tag{43}$$

Substituting this into Eq. 42 and affecting both parts of the equation by the operator $1 - \mathcal{B}\theta/2$ gives

$$\left(1 - \frac{1}{2}\mathcal{B}\theta\right) C^{k+1}(x) = \left(1 + \frac{1}{2}\mathcal{B}\theta\right) C^k(x). \tag{44}$$

This is a discrete equation which approximates the original solution given in Eq. 42 with the second order in θ. One can easily recognize in this scheme a famous Crank-Nicolson scheme.

We do not want to invert the operator $\mathcal{A}_x^-$ in order to compute the operator $\mathcal{B}$ because $\mathcal{B}$ is an integral operator. Therefore, we will apply the operator $\mathcal{A}_x^-$ to the both sides of Eq. 44. The resulting equation is a pure differential equation and reads

$$\left(\mathcal{A}_x^- - \frac{\sqrt{V_R}}{4}\theta\right) C^{k+1}(x) = \left(\mathcal{A}_x^- + \frac{\sqrt{V_R}}{4}\theta\right) C^k(x). \tag{45}$$

Let us work with the operator $\mathcal{A}_x^-$ (for the operator $\mathcal{A}_x^+$ all corresponding results can be obtained in a similar way). The operator $\mathcal{A}_x^-$ contains derivatives in x up to the order $p+1$. If one uses a finite difference representation of these derivatives the resulting matrix in the rhs of Eq. 45 is a band matrix. The number of diagonals in the matrix depends on the value of $p = -(1+\alpha_R) > 0$. For central difference approximation of derivatives of order d in x with the order of approximation q the matrix will have at least $l = d+q$ diagonals, where it appears that $d+q$ is necessarily an odd number (Eberly 2008). Therefore, if we consider a second order approximation in x, i.e. $q = 2$ in our case the number of diagonals is $l = p+3 = 2-\alpha_R$.

As the rhs matrix $\mathcal{D} \equiv \mathcal{A}_x^- - \sqrt{V_R}\theta/4$ is a band matrix the solution of the corresponding system of linear equations in Eq. 45 could be efficiently obtained using a modern technique (for instance, using a ScaLAPACK package).[2] The computational cost for the LU factorization of an N-by-N matrix with lower bandwidth P and upper bandwidth Q is $2NPQ$ (this is an upper bound) and storage-wise—$N(P+Q)$. So in our case of the symmetric matrix the cost is $(1-\alpha_R)^2 N/2$ performance-wise and $N(1-\alpha_R)$ storage-wise. This means that the complexity of our algorithm is still $O(N)$ while the constant $(1-\alpha_R)^2/2$ could be large.

A typical example could be if we solve our PDE using an x-grid with 300 nodes, so $N = 300$. Suppose $\alpha_R = -10$. Then the complexity of the algorithm is $60N = 18000$. Compare this with the FFT algorithm complexity which is $(34/9)2N\log_2(2N) \approx 20900$,[3] one can see that our algorithm is of the same speed as the FFT.

The case $m = 2$ could be achieved either using symmetric (2,2) or diagonal (1,2) Padé approximations of the operator exponent. The (1,2) Padé approximation reads

$$e^{\mathcal{B}\theta} = \frac{1+\mathcal{B}\theta/3}{1-2\mathcal{B}\theta/3+\mathcal{B}^2\theta^2/6}, \tag{46}$$

and the corresponding finite difference scheme for the solution of Eq. 42 is

$$\begin{aligned}&\left[(\mathcal{A}_x^-)^2 - \frac{1}{3}\sqrt{V_R}\theta\mathcal{A}_x^- + \frac{1}{24}V_R\theta^2\right]C^{k+1}(x)\\ &= \mathcal{A}_x^-\left[\mathcal{A}_x^- + \frac{1}{6}\sqrt{V_R}\theta\right]C^k(x).\end{aligned} \tag{47}$$

which is of the third order in θ. The (2,2) Padé approximation is

$$e^{\mathcal{B}\theta} = \frac{1+\mathcal{B}\theta/2+\mathcal{B}^2\theta^2/12}{1-\mathcal{B}\theta/2+\mathcal{B}^2\theta^2/12}, \tag{48}$$

[2] see http://www.netlib.org/scalapack/scalapack_home.html.

[3] We use $2N$ instead of N because in order to avoid undesirable wrap-round errors a common technique is to embed a discretization Toeplitz matrix into a circulant matrix. This requires to double the initial vector of unknowns.

and the corresponding finite difference scheme for the solution of Eq. 42 is

$$\left[(\mathcal{A}_x^-)^2 - \frac{1}{4}\sqrt{V_R}\theta\mathcal{A}_x^- + \frac{1}{48}V_R\theta^2\right]C^{k+1}(x) = \left[(\mathcal{A}_x^-)^2 + \frac{1}{4}\sqrt{V_R}\theta\mathcal{A}_x^- + \frac{1}{48}V_R\theta^2\right]C^k(x), \tag{49}$$

which is of the fourth order in θ.

Matrix of the operator $(\mathcal{A}_x^-)^2$ has $2l-1$ diagonals, where l is the number of diagonals of the matrix $\mathcal{A}_x^-$. Thus, the finite difference equations (47) and (49) still have band matrices and could be efficiently solved using an appropriate technique.

4.2 Stability Analysis

Stability analysis of the derived finite difference schemes could be provided using a standard von-Neumann method. Suppose that operator $\mathcal{A}_x^-$ has eigenvalues ζ which belong to continuous spectrum. Any finite difference approximation of the operator $\mathcal{A}_x^- - FD(\mathcal{A}_x^-)$—transforms this continuous spectrum into some discrete spectrum, so we denote the eigenvalues of the discrete operator $FD(\mathcal{A}_x^-)$ as $\zeta_i, i = 1, N$, where N is the total size of the finite difference grid.

Now let us consider, for example, the Crank-Nicolson scheme given in Eq. 45. It is stable if in some norm $\|\cdot\|$

$$\left\|\left(\mathcal{A}_x^- - \frac{\sqrt{V_R}}{4}\theta\right)^{-1}\left(\mathcal{A}_x^- + \frac{\sqrt{V_R}}{4}\theta\right)\right\| < 1. \tag{50}$$

It is easy to see that this inequality obeys when all eigenvalues of the operator $\mathcal{A}_x^-$ are negative. However, based on the definition of this operator given in the Proposition 2, it is clear that the central finite difference approximation of the first derivative does not give rise to a full negative spectrum of eigenvalues of the operator $FD(\mathcal{A}_x^-)$. So below we define a different approximation.

Case $\alpha_{\mathbf{R}} < \mathbf{0}$. Therefore, in this case we will use a one-sided forward approximation of the first derivative which is a part of the operator $\left(\nu_R - \frac{\partial}{\partial x}\right)^{\alpha_R}$. Define $h = (x_{\max} - x_{\min})/N$ to be the grid step in the x-direction, N is the total number of steps, $x_{\min}$ and $x_{\max}$ are the left and right boundaries of the grid. Also define $c_i^k = C^k(x_i)$. To make our method to be of the second order in x we use the following numerical approximation.

$$\frac{\partial C^k(x)}{\partial x} = \frac{-C_{i+2}^k + 4C_{i+1}^k - 3C_i^k}{2h} + O(h^2) \tag{51}$$

Matrix of this discrete difference operator has the following form

$$M_f = \frac{1}{2h}\begin{pmatrix} -3 & 4 & -1 & 0 & \dots 0 \\ 0 & -3 & 4 & -1 & \dots 0 \\ 0 & 0 & -3 & 4 & \dots 0 \\ \dots & \dots & \dots & \dots & \dots \\ 0 & 0 \dots & 0 & 0 & -3 \end{pmatrix} \tag{52}$$

All eigenvalues of M_f are equal to $-3/(2h)$.

To get a power of the matrix M we use its spectral decomposition, i.e. we represent it in the form $M = EDE'$, where D is a diagonal matrix of eigenvalues d_i, $i = 1, N$ of the matrix M, and E is a matrix of eigenvectors of the matrix M. Then $M^{p+1} = ED^{p+1}E'$, where the matrix D^{p+1} is a diagonal matrix with elements d_i^{p+1}, $i = 1, N$. Therefore, the eigenvalues of the matrix $\left(\nu_R - \frac{\partial}{\partial x}\right)^{\alpha_R}$ are $[\nu_R + 3/(2h)]^{\alpha_R}$. And, consequently, the eigenvalues of the matrix $\mathbb{B}$ are

$$\zeta_{\mathbb{B}} = \sqrt{V_R}\lambda_R\Gamma(-\alpha_R)\left\{[\nu_R + 3/(2h)]^{\alpha_R} - \nu_R^{\alpha_R}\right\}. \tag{53}$$

As $\alpha_R < 0$ and $\nu_R > 0$ it follows that $\zeta_{\mathbb{B}} < 0$. Rewriting Eq. 44 in the form

$$C^{k+1}(x) = \left(1 - \frac{1}{2}\mathcal{B}\theta\right)^{-1}\left(1 + \frac{1}{2}\mathcal{B}\theta\right)C^k(x), \tag{54}$$

and taking into account that $\zeta_{\mathbb{B}} < 0$ we arrive at the following result

$$\left\|\left(1 - \frac{1}{2}\mathcal{B}\theta\right)^{-1}\left(1 + \frac{1}{2}\mathcal{B}\theta\right)\right\| < 1. \tag{55}$$

We also obey the condition $\mathbb{R}\left(\nu_R - \frac{\partial}{\partial x}\right) > 0$. Thus, our numerical method is unconditionally stable.

Case $\alpha_{\mathbf{L}} < \mathbf{0}$ In this case we will use a one-sided backward approximation of the first derivative in the operator $\left(\nu_L + \frac{\partial}{\partial x}\right)^{\alpha_L}$ which reads

$$\frac{\partial C^k(x)}{\partial x} = \frac{3C_i^k - 4C_{i-1}^k + C_{i-2}^k}{2h} + O(h^2) \tag{56}$$

Matrix of this discrete difference operator has the following form

$$M_b = \frac{1}{2h}\begin{pmatrix} 3 & 0 & 0 & 0 & \dots 0 \\ -4 & 3 & 0 & 0 & \dots 0 \\ 1 & -4 & 3 & 0 & \dots 0 \\ \dots & \dots & \dots & \dots & \dots \\ 0 & 0 \dots & 1 & -4 & 3 \end{pmatrix} \tag{57}$$

All eigenvalues of M_b are equal to $3/(2h)$. Then doing in a similar way as above we can show that the eigenvalues of the operator $\mathbb{B}$ read

$$\zeta_{\mathbb{B}} = \sqrt{V_L}\lambda_L \Gamma(-\alpha_L)\left\{[\nu_L + 3/(2h)]^{\alpha_L} - \nu_L^{\alpha_L}\right\}. \tag{58}$$

As $\alpha_L < 0$ and $\nu_L > 0$ it follows that $\zeta_{\mathbb{B}} < 0$, $\mathbb{R}\left(\nu_L + \frac{\partial}{\partial x}\right) > 0$, and the numerical method in this case is unconditionally stable.

4.3 $\alpha \in \mathbb{R}$—Interpolation

Before we discuss some alternative approaches (see next sections) let us consider a simple way how to solve pure jump equations in the general case $\alpha \in \mathbb{R}$. We already showed how to transform our PIDEs to some pseudo-parabolic PDE and then solve them using a finite difference approach if $\alpha \in \mathbb{Z}$. A simple observation shows that having results computed for $\alpha \in \mathbb{Z}$ we may then interpolate them with the second order in α to obtain the solution at any $\alpha \in \mathbb{R}$. To make sure this is consistent we prove the following proposition.

Proposition 5 *Both integrals in Eq. 21 are continuous in α at $\alpha < 2$.*

Proof See Appendix.

4.4 Numerical Examples

Here we present results of various numerical tests aimed to compare our method with the standard FFT approach. In doing so main attention is drawn to a relative performance and accuracy of both methods, rather than to economic treatment of the results. That is done for two reasons. First, we apply our method to the jump model which has already received a significant attention in the literature. See a short discussion and references at the beginning of Sect. 3. Second, as was already mentioned, we consider only one step (jumps) in the whole multi-step splitting algorithm. Therefore, to compute, e.g. option prices under this model we need to implement all other steps as well. This subject is out of scope of this paper and is discussed in more detail in Itkin and Carr (2011). There exists also a wide literature (see Sect. 1) where this comparison is done using the FTT based calculation of the jump integrals. Therefore, we don't expect to obtain any new results in this way, but just to provide a new and efficient algorithm to solve the jump-diffusion equations.

Below two series of numerical experiments are described. In the first series we solve the equation

$$\frac{\partial}{\partial \tau} C(x,\tau) = \int_0^\infty C(x+y,\tau)\lambda_R \frac{e^{-\nu_R|y|}}{|y|^{1+\alpha_R}} dy, \quad \alpha_R < -1 \tag{59}$$

by using FFT and the finite difference scheme constructed based on computation of Eq. 59 with $\alpha_R \in \mathbb{Z}$ and interpolation as it was described in the above.

We solve an initial problem despite it is easy to consider a boundary problem as well. As an example we consider a put option with time to maturity $T = 30$ days.[4] As the terminal condition (we compute the solution backward in time) we choose a Black-Scholes put value at $\tau = 0$ where the interest rate is $r = 0.01$, the volatility is 0.1 and the strike is $K = 100$. We create a uniform grid in time with $N_t = 50$ nodes, so $\theta = T/N_t$ is the step in time.

FFT. To apply an FFT approach we first select a domain in x space where the values of function $C(x, \tau)$ are of our interest. Suppose this is $x \in (-x_*, x_*)$. We define a uniform grid in this domain which contains N points: $x_1 = -x_*, x_2, \ldots, x_{N-1}, x_N = x_*$ such that $x_i - x_{i-1} = h, i = 2 \ldots N$. We then approximate the integral in the rhs of Eq. 59 with the first order of accuracy in h as

$$\int_0^\infty C(x+y,\tau)\lambda_R \frac{e^{-\nu_R|y|}}{|y|^{1+\alpha_R}}dy = \frac{h}{2}\sum_{j=1-i}^{N-i} C_{i+j}(\tau) f_j, \quad f_j \equiv \lambda_R \frac{e^{-\nu_R|x_j|}}{|x_j|^{1+\alpha_R}} + O(h^2). \tag{60}$$

This approximation means that we have to extend our computational domain to the left up to $x_{1-N} = x_1 - hN$.

The matrix $|f|$ is a Toeplitz matrix. Using FFT directly to compute a matrix-vector product in Eq. 60 will produce a wrap-round error that significantly lowers the accuracy. Therefore a standard technique is to embed this Toeplitz matrix into a circulant matrix $\mathcal{F}$ which is defined as follows. The first row of F is

$$F_1 = (f_0, f_1, \ldots, f_{N-1}, 0, f_{1-N}, \ldots, f_{-1}),$$

and others are generated by permutation (see, for instance, Zhang and Wang 2009). We also define a vector

$$\hat{C} = [C_1(\tau), \ldots C_N(\tau), \underbrace{0, \ldots, 0}_{N}]^T.$$

Then the matrix-vector product in the rhs equation (60) is given by the first N rows in the vector $V = \text{ifft}(\text{fft}(F_1) * \text{fft}(\hat{C}))$, where fft and ifft are the forward and inverse discrete Fourier transforms as they are defined, say in Matlab. In practice, an error at edge points close to x_1 and x_N is higher, therefore it is useful first to add some points left to x_1 and right to x_N and then apply the above described algorithm to compute the integral. We investigated some test problems, for instance, where the function C was chosen as $C(x) = x$ so the integral can be computed analytically. Based on the obtained results we found that it is useful to extend the computational domain adding $N/2$ points left to x_1 and right to x_N that provides an accurate solution in the domain $x_1, \ldots, x_N$.

[4] We keep same notation for the put option value which is $C(x, \tau)$, as this comparison means basically to compare two numerical methods rather than provide some deep economic meaning.

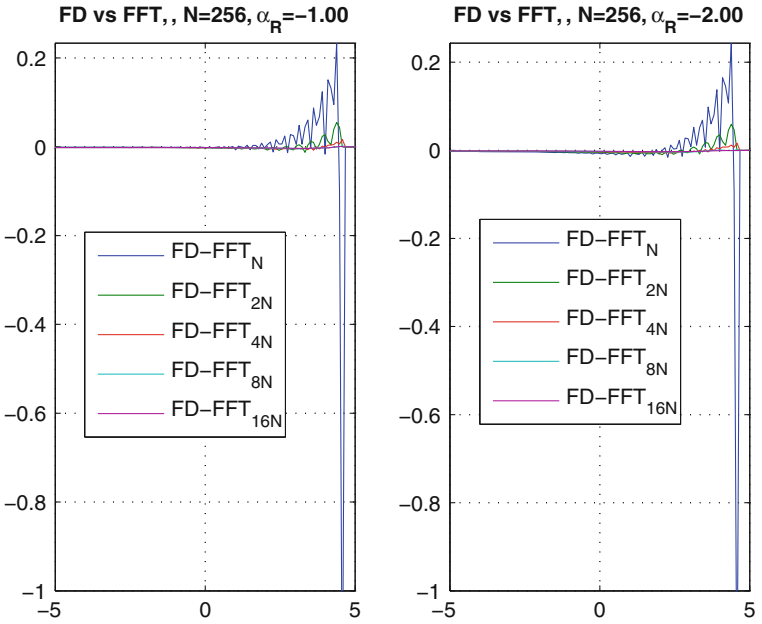

Fig. 1 Difference (FD–FFT) in solutions of Eq. 59 as a function of x obtained using our FD and an explicit Euler scheme in time where the jump integral is computed using FFT. $\alpha_R = -1, -2$

The drawback of this is that the resulting circulant matrix has $4N \times 4N$ elements that increases the computational work by 4 times ($4N \log_2(4N) \approx 4(N \log_2 N)$).

In our calculations we used $x_* = 20$, $h = 2x_*/N$ regardless of the value of N which varies in the experiments. Then we extended the domain to $x_1 = -x_* - h(N/2-1)$, $x_N = x_* + h(N/2+1)$, and so this doubles the originally chosen value of N, i.e. $N_{new} = 2N$. But the final results were analyzed at the domain $x \in (-x_*, x*)$.

Integrating Eq. 59 in time we use an explicit Euler scheme of the first order which is pretty fast. This is done in order to provide the worst case scenario for the below FD scheme. Thus, if our FD scheme is comparable in speed with FFT in this situation it will even better if some other more accurate integration schemes are applied together with the FFT.

FD. We build a fixed grid in the x space by choosing $S_{\min} = 10^{-8}$, $S_{\max} = 500$, $x_1 = \log(S_{\min})$, $x_N = \log(S_{\max})$, $h = (x_N - x_1)/N$, $N = 256$. A one-sided forward approximation of the first derivative was used as it is defined in Eq. 51 to approximate the operator in Eq. 59. In the particular case considered here in our experiments $V_R \equiv 1$, and the compensators in Eq. 21 are not considered, because they could be integrated out at $\alpha_R < 0$ and added to the diffusion terms. The Crank-Nicolson scheme Eq. 54 was applied to integrate Eq. 59 in time.

Results The first series of tests was provided when $\alpha_R \in \mathbb{Z}$ and $\nu_R = 1$, $\lambda_R = 0.2$. The results of this series are presented in Figs. 1 and 2. The corresponding execution time is given in Table 1.

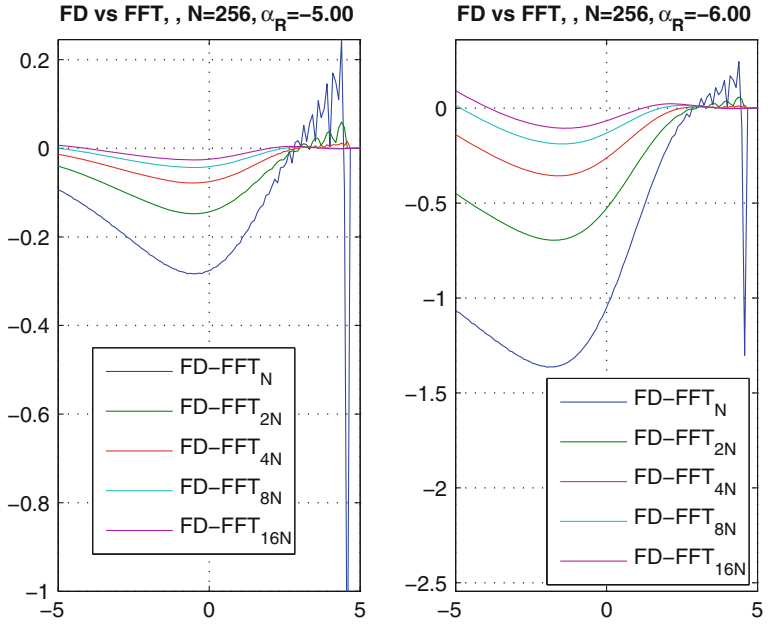

Fig. 2 Same as in Fig. 1. $\alpha_R = -5, -6$

In case $\alpha_R = -1$ in Fig. 1 the FFT solution computed with $N = 256$ provides a relatively big error which disappears with N increasing. It is clear, because the Crank-Nicolson scheme is of the second order in h while the approximation Eq. 60 of the integral is of the first order in h. Numerical values of the corresponding steps in the described experiments are given in Table 2.

Therefore, $h_{FD}^2 \approx h_{FFT_{16}}$. Actually, the difference between the FD solution with $N_{FD} = 256$ and the FFT one with $N = 4N_{FD}$ is almost negligible. However, the FD solution is computed almost 13 times faster. Even the FFT solution with $N = N_{FD}$ is 10 times slower than the FD one.[5]

For $\alpha_R = -2$ in Fig. 1 we see almost the same picture. For $\alpha_R = -5$ speed characteristics of both solutions are almost same while the accuracy of the FD solution decreases. This is especially pronounced for $\alpha_R = -6$ in Fig. 2 at low values of $x < -7$ (which lies outside of the graph). The problem is that when α_R decreases the eigenvalues of matrix $\mathcal{B}$ in Eq. 44 grow significantly (in our tests at $\alpha_R = -6$ the eigenvalues are of order of 10^7), so in Eq. 55 the norm of the matrix is very close to 1. Thus, the FD method becomes just an A-stable. However, a significant difference is observed mostly at very low values of x which correspond to the spot price $S = \exp(x)$ close to zero. For a boundary problem this effect is partly dumped by the boundary condition at the low end of the domain.

The second series of tests deals with $\alpha_R \in \mathbb{R}$ using the same parameters $\nu_R = 1, \lambda_R = 0.2$. The results of this series are presented in Figs. 3 and 4. Four

[5] It actually uses $4N$ points as it was already discussed.

Table 1 Relative time FD(N)/FFT(kN) of computations for $\alpha \in \mathbb{Z}$ and $N = 256$ obtained in the numerical experiments

α_R	FD (s)	k				
		1	2	4	8	16
−1	0.0257	0.0657	0.0644	0.0543	0.0511	0.0338
−2	0.0273	0.0708	0.0686	0.0625	0.0543	0.0387
− 5	0.0283	0.0733	0.0682	0.0582	0.0555	0.0387
−6	0.0280	0.0720	0.0645	0.0637	0.0550	0.0379

Table 2 Grid steps h used in the numerical experiments

	FD_{256}	FFT_{256}	FFT_{512}	FFT_{1024}	FFT_{2048}	FFT_{4096}
h	0.096	0.1563	0.078	0.039	0.0195	0.00977

Table 3 Relative time FD(N)/FFT(kN) of computations for $\alpha \in \mathbb{R}$ and $N = 256$ obtained in the numerical experiments

α_R	FD (s)	k				
		1	2	4	8	16
−0.5	0.1336	0.3330	0.3129	0.2847	0.2243	0.1417
−1.5	0.1289	0.3023	0.2958	0.2751	0.2374	0.1462
−3.5	0.1274	0.3280	0.3179	0.2801	0.2416	0.1703
−5.5	0.1379	0.3459	0.3408	0.2984	0.2553	0.1909

point cubic interpolation is used to compute the value of $C(x, \tau)$ at real α_R using the closest four integer values of α_R. The corresponding execution time is given in Table 3.

It is seen that cubic interpolation provides pretty good approximation to the solution which is comparable with the FFT method in the accuracy and is faster in speed. Again, as we already discussed at $\alpha_R < 5$ the accuracy of the FD scheme drops down even for $\alpha_R \in \mathbb{R}$, therefore the same picture is observed for $\alpha_R \in \mathbb{R}$.

At $-1 < \alpha_R < 0$ (see Fig. 3) the difference between FD and FFT solutions surprisingly increases with N, used in the FFT method, increasing. To better understand what is the reason of that we fulfilled a test calculation of the integral in the rhs of Eq. 59 when $C(x, \tau)$ is a known function, namely $C(x, \tau) \equiv x$. In this case this integral can be computed analytically which gives

$$\int_0^\infty (x + y) \frac{e^{-\nu_R |y|}}{|y|^{1+\alpha_R}} dy = (x\nu_R - \alpha_R)\nu_R^{\alpha_R - 1}\Gamma(-\alpha_R). \tag{61}$$

Then we apply the above described FFT approach and compare the numerical solution with the analytical one. The results of this test are given in Fig. 5. It is seen that FFT algorithm used in our calculations doesn't provide a good approximation to the

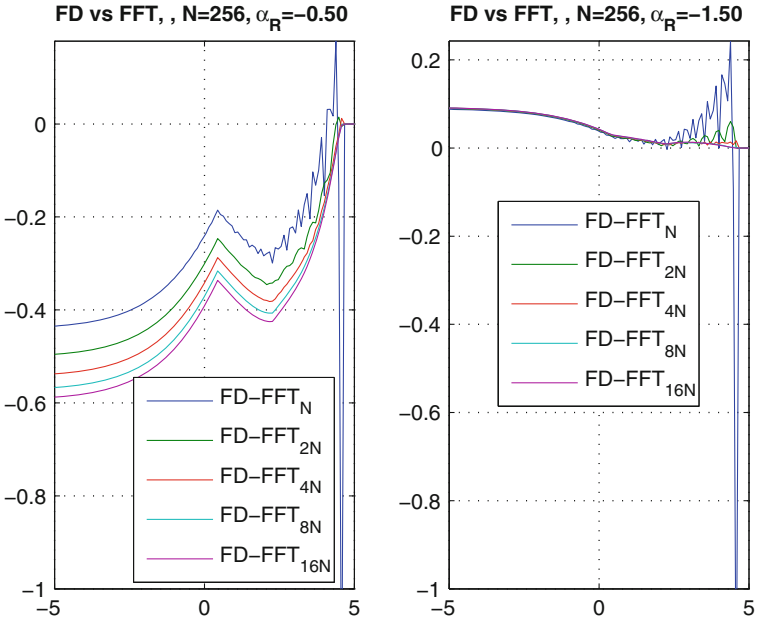

Fig. 3 Difference (FD–FFT) in solutions of Eq. 59 as a function of x at $\alpha_R \in \mathbb{R}$ obtained using our FD and interpolation and an explicit Euler scheme in time where the jump integral is computed using FFT. $\alpha_R = -0.5, -1.5$

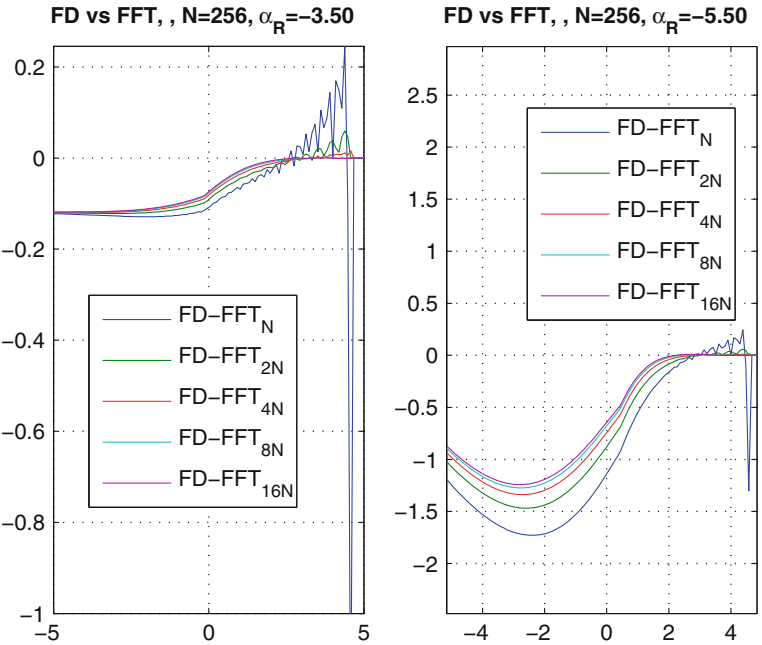

Fig. 4 Same as in Fig. 3. $\alpha_R = -3.5, -5.5$

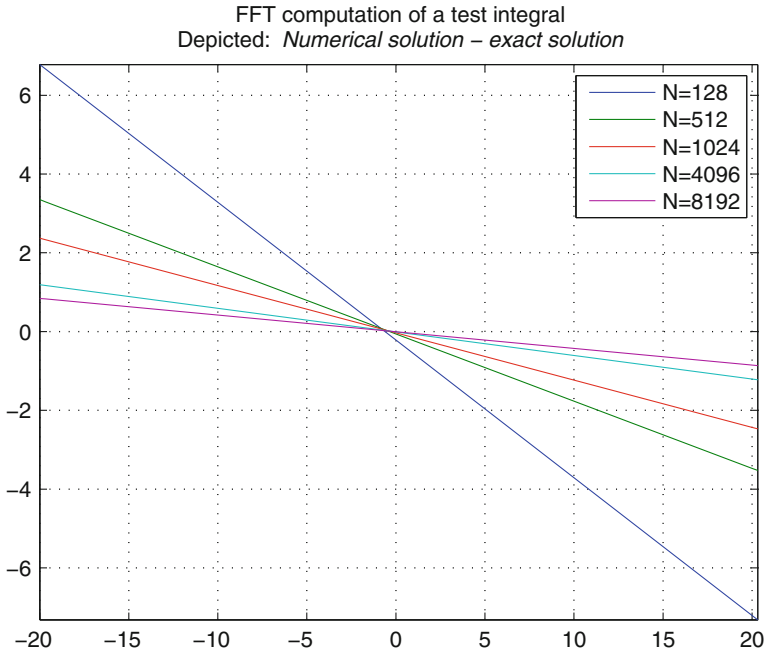

Fig. 5 FFT computation of a test integral in Eq. 61

analytical solutions at low N. So we expect this behavior of the FFT method occurred in our numerical experiments at $\alpha_R = -0.5$, but this doesn't explain the observed effect.

A plausible explanation is that at α_R close to 0 the integral kernel becomes singular. That is why in Cont and Voltchkova (2003) the part of the infinitesimal generator corresponding to small jumps is approximated by a differential operator of second order (additional diffusion component). As we didn't use this technique here, an increase of N forces the distance between $y = 0$ and the closest FFT node boundary to become smaller, thus the kernel becomes larger.

The other reason for the FD solution to differ from the FFT solution is that at $-1 < \alpha_R < 0$ we don't use the option values computed at $\alpha_R = 0$ (remember, this is a special case that was discussed earlier). Thus, instead of interpolation we use extrapolation that certainly decreases the accuracy of the FD solution. We will resolve this problem in the next section.

At the end of this section we present the option values computed using such a scheme as a function of x obtained in the same test (Fig. 6).

5 General Case

In the general case $\alpha \in \mathbb{R}, \alpha \leq -1$ Propositions 1 and 2 could be generalized. To do that we need to replace the binomial coefficients with that defined via the Gamma function, and also replace usual derivatives with a properly defined fractional derivatives.

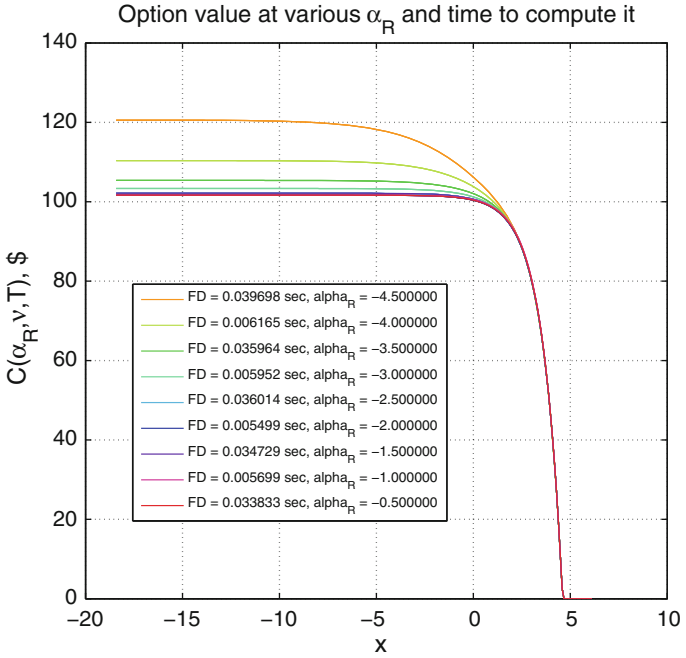

Fig. 6 Option values computed using such a scheme as a function of x obtained in the same test

Proposition 6 *Assume that in Eq. 27* $\alpha \in \mathbb{R}, \alpha \leq -1$. *Then the solution of Eq. 27 with respect to* $\mathcal{A}_x^+$ *is*

$$\mathcal{A}_x^+ = \frac{1}{\lambda\Gamma(p+1)}\left(\nu + \frac{\partial}{\partial x}\right)^{p+1} \equiv \frac{1}{\lambda\Gamma(p+1)}\left[\sum_{i=0}^{\infty} C_i^{p+1}\nu^{p+1-i}\frac{\partial^i}{\partial x^i}\right],$$
$$p \equiv -(1+\alpha) \geq 0,$$

where C_i^{p+1} *are the generalized binomial coefficients which could be expressed via the Gamma function, and fractional derivatives are understood in the Riemann-Liouville sense (Oldham and Spanier 1974).*

The proof is given in Appendix. For the operator $\mathcal{A}_x^-$ the proof is similar.

This means that the whole analysis of the previous sections made in the case $\alpha \in \mathbb{Z}$ is still valid for arbitrary $\alpha \in \mathbb{R}, \alpha < 0$. Moreover, we could now extend this proof for the whole range of $\alpha < 2$. In order to do that we have to consider the whole integrals in Eq. 21. As this is well-known for jumps with infinite activity or infinite variation the second and third integrands can not be integrated out, otherwise the integral does not converge.

If we apply the second transformation to the first equation in Eq. 24 the result is given by the following proposition.

Proposition 7 *The PIDE*

$$\frac{\partial}{\partial\tau}C(x,V_R,V_L,\tau) = \sqrt{V_R}\int_0^\infty\left[C(x+y,V_R,V_L,\tau)-C(x,V_R,V_L,\tau) - \frac{\partial}{\partial x}C(x,V_R,V_L,\tau)(e^y-1)\right]\lambda_R\frac{e^{-\nu_R|y|}}{|y|^{1+\alpha_R}}dy \tag{62}$$

is equivalent to PDE

$$\frac{\partial}{\partial\tau}C(x,V_R,V_L,\tau) = \sqrt{V_R}\lambda_R\Gamma(-\alpha_R)\left\{\left(\nu_R-\frac{\partial}{\partial x}\right)^{\alpha_R}-\nu_R^{\alpha_R}+\left[\nu_R^{\alpha_R}-(\nu_R-1)^{\alpha_R}\right]\frac{\partial}{\partial x}\right\}$$
$$C(x,V_R,V_L,\tau),\mathbb{R}(\alpha_R)<2,\ \mathbb{R}(\nu_R-\partial/\partial x)>0,\ \mathbb{R}(\nu_R)>1. \tag{63}$$

In special cases this equation changes to

$$\frac{\partial}{\partial\tau}C(x,V_R,V_L,\tau) = \sqrt{V_R}\lambda_R\left\{\log(\nu_R)-\log\left(\nu_R-\frac{\partial}{\partial x}\right)+\log\left(\frac{\nu_R-1}{\nu_R}\right)\frac{\partial}{\partial x}\right\}$$
$$C(x,V_R,V_L,\tau)\alpha_R = 0,\mathbb{R}(\nu_R-\partial/\partial x)>0,\mathbb{R}(\nu_R)>1, \tag{64}$$

and

$$\frac{\partial}{\partial\tau}C(x,V_R,V_L,\tau) = \sqrt{V_R}\lambda_R\left\{-\nu_R\log\nu_R+(\nu_R-\frac{\partial}{\partial x})\log\left(\nu_R-\frac{\partial}{\partial x}\right) + \left[\nu_R\log\nu_R-(\nu_R-1)\log(\nu_R-1)\right]\frac{\partial}{\partial x}\right\}C(x,V_R,V_L,\tau)$$
$$\alpha_R = 1,\mathbb{R}(\partial/\partial x)<0,\mathbb{R}(\nu_R)>1, \tag{65}$$

where logarithm of the differential operator is defined in a sense of Bakas et al. (1993).

Proof We again use the shift operator introduced in Eq. 98 to rewrite Eq. 62 as

$$\frac{\partial}{\partial\tau}C(x,V_R,V_L,\tau) = \mathcal{B}_1C(x,V_R,V_L,\tau)$$
$$\mathcal{B}_1 \equiv \sqrt{V_R}\int_0^\infty\left[\exp\left(y\frac{\partial}{\partial x}\right)-1-(e^y-1)\frac{\partial}{\partial x}\right]\lambda_R\frac{e^{-\nu_R|y|}}{|y|^{1+\alpha_R}}dy \tag{66}$$

Formal integration could be fulfilled if we treat a differential operator $\frac{\partial}{\partial x}$ as a parameter. As it could be verified the result is that given in Eq. 63. Same method is used to prove the formulae given in the special cases $\alpha_R = 0$ and $\alpha_R = 1$. □

Also notice that at $\alpha_R = 0$ from the very beginning the last term in Eq. 62 can be moved from the integral to the diffusion part of Eq. 21 because the remaining kernel converges at $y = 0$. If we do so, at this special case the integrated equation transforms to

$$\frac{\partial}{\partial\tau}C(x,V_R,V_L,\tau) = \sqrt{V_R}\lambda_R\left\{\log(\nu_R) - \log\left(\nu_R - \frac{\partial}{\partial x}\right)\right\}C(x,V_R,V_L,\tau)$$
$$\alpha_R = 0, \mathbb{R}(\nu_R - \partial/\partial x) > 0, \mathbb{R}(\nu_R) > 0, \tag{67}$$

This form is more useful as we show later when elaborating a numerical method to solve it.

The same approach could be utilized for the second equation in Eq. 24, and the result is given by the following proposition.

Proposition 8 *The PIDE*

$$\frac{\partial}{\partial\tau}C(x,V_R,V_L,\tau) = \sqrt{V_L}\int\limits_{-\infty}^{0}\Big[C(x+y,V_R,V_L,\tau) - C(x,V_R,V_L,\tau)$$
$$-\frac{\partial}{\partial x}C(x,V_R,V_L,\tau)(e^y-1)\Big]\lambda_L\frac{e^{-\nu_L|y|}}{|y|^{1+\alpha_L}}dy \tag{68}$$

is equivalent to PDE

$$\frac{\partial}{\partial\tau}C(x,V_R,V_L,\tau)$$
$$= \sqrt{V_L}\lambda_L\Gamma(-\alpha_L)\left\{\left(\nu_L + \frac{\partial}{\partial x}\right)^{\alpha_L} - \nu_L^{\alpha_L} + \left[\nu_L^{\alpha_L} - (\nu_L+1)^{\alpha_L}\right]\frac{\partial}{\partial x}\right\}$$
$$C(x,V_R,V_L,\tau), \mathbb{R}(\alpha_L) < 2,\ \mathbb{R}(\nu_L + \partial/\partial x) > 0,\ \mathbb{R}(\nu_L) > 0. \tag{69}$$

In special cases this equation changes to

$$\frac{\partial}{\partial\tau}C(x,V_R,V_L,\tau) = -\sqrt{V_L}\lambda_L\left\{\log\left(\nu_L + \frac{\partial}{\partial x}\right) - \log(\nu_L) - \log\left(\frac{\nu_L+1}{\nu_L}\right)\frac{\partial}{\partial x}\right\}$$
$$\alpha_L = 0,\ \mathbb{R}(\nu_L + \partial/\partial x) > 0,\ \mathbb{R}(\nu_L) > 0, \tag{70}$$

and

$$\frac{\partial}{\partial\tau}C(x,V_R,V_L,\tau) = \sqrt{V_L}\lambda_L\left\{-\nu_L\log\nu_L + \left[\nu_L\log\nu_L - (\nu_L+1)\log(\nu_L+1)\right]\right.$$
$$\left.\times\ \frac{\partial}{\partial x} + (\nu_L + \frac{\partial}{\partial x})\log\left(\nu_L + \frac{\partial}{\partial x}\right)\right\}C(x,V_R,V_L,\tau)$$
$$\alpha_R = 1,\ \mathbb{R}(\partial/\partial x) < 0,\ \mathbb{R}(\nu_L) > 0, \tag{71}$$

where logarithm of the differential operator is defined in a sense of Bakas et al. (1993).

Proof The proof is similar to that given in the Proposition 7. □

Again at $\alpha_L = 0$ we can move out the last term in Eq. 62 from the integral to the diffusion part of Eq. 21 because the remaining kernel converges at $y = 0$. If we do so, at this special case the integrated equation transforms to

$$\frac{\partial}{\partial\tau}C(x, V_R, V_L, \tau) = -\sqrt{V_L}\lambda_L \left\{\log\left(\nu_L + \frac{\partial}{\partial x}\right) - \log(\nu_L)\right\} \tag{72}$$
$$\alpha_L = 0,\ \mathbb{R}(\nu_L + \partial/\partial x) > 0,\ \mathbb{R}(\nu_L) > 0,$$

We will use this form later when elaborating a numerical method to solve this equation.

It is important to underline that the integration in the Proposition 7 for positive jumps could be done if $\mathbb{R}(\nu_R) > 1$ while in the Proposition 8 for negative jumps - if $\mathbb{R}(\nu_L) > 0$. In the special cases $\alpha_R = 1$ this limit could be extended to $\mathbb{R}(\nu_R) > 0$, however it gives rise to a complex values of the coefficients in the rhs of Eq. 71. Therefore, we keep the above constraint $\mathbb{R}(\nu_R) > 1$ unchanged in this case as well.

Similar representations were obtained first in Boyarchenko and Levendorskii (2002) and later in Cartea and del Castillo-Negrete (2007) using a characteristic function approach. For instance, the latter authors considered several Lévy processes with known characteristic function, namely LS, CGMY or KoBoL. Then using Fourier transform they managed to convert the governing PIDE (same type as Eq. 21 but for the Black-Scholes model with jumps) to a fractional PDE. In their notation our operator $\mathcal{A}_1$ is represented as

$$\mathcal{A}_1 \propto (-1)^{\alpha_R} e^{\nu_R}\ {}_x\mathbb{D}_{\infty}^{\alpha_R}\left(e^{-\nu_R}C(x,t)\right), \tag{73}$$

and operator $\mathcal{A}_2$ as

$$\mathcal{A}_2 \propto e^{\nu_L}\ {}_{\infty}\mathbb{D}_{x}^{\alpha_L}\left(e^{-\nu_L}C(x,t)\right), \tag{74}$$

So to compare we have to note that aside of the different method of how to derive these equations our main contribution in this paper is:

1. Special cases $\alpha_r = 0, 1, \alpha_l = 0, 1$ are not considered in Cartea and del Castillo-Negrete (2007). In Boyarchenko and Levendorskii (2002) a corresponding characteristic function of the KoBoL process was obtained in all cases for $\alpha \leq 1$. However, the authors did not consider numerical solution of the fractional PDE. In this paper we derive a fractional PDE for all $\alpha < 2$ and propose a numerical method for their solution.
2. We proposed the idea of solving FPDE with real $\alpha_R \leq 0, \alpha_L \leq 0$ by using interpolation between option prices computed for the closest integer values of α_R, α_L. For the latter we first used to transform the fractional equation into a pseudo-parabolic equation. Then for the solution of this PPDE an efficient FD scheme is constructed that results in LU factorization of the band matrix.

3. Also jumps up and down are considered separately so the model in use (SSM) is slightly different from the model considered in Cartea and del Castillo-Negrete (2007).
4. In Cartea and del Castillo-Negrete (2007) a Crank-Nicolson type numerical scheme was proposed to solve the obtained FPDE in time while discretization in space was done using the Grunwald–Letnikov approximation which is of the first order in space. Here for fractional equations with $2 > \alpha_R > 0, 2 > \alpha_L > 0$ we obtain the solution using our new scheme which preserves the second order approximation in time and space.
5. As it is known from recent papers (Abu-Saman and Assaf 2007; Meerschaert and Tadjeran 2004; Tadjeran et al. 2006; Meerschaert and Tadjeran 2006; Sousa 2008), a standard Grunwald–Letnikov approximation leads to unconditionally unstable schemes. To improve this a shifted Grunwald–Letnikov approximation was proposed which allows construction of the unconditionally stable scheme of the first order in space.[6] Here we use a different approach to derive the unconditionally stable scheme of higher order.
6. We show that when considering jumps with finite activity and finite variation despite it is a common practice to integrate out all Lévy compensators in Eq. 21 in the integral terms this breaks the stability of the scheme at least for the fractional PDE. Therefore, in order to construct the unconditionally stable scheme one must keep some other terms under the integrals. To resolve this in Cartea and del Castillo-Negrete (2007) the authors were compelled to change their definition of the fractional derivative (see below).
7. Our approach could be easily generalized for a time-dependent Lévy density.

6 Numerical Method

Let us consider a general case which is given by Eqs. 63 and 69.[7] We first discuss how to construct an unconditionally stable scheme of the second order in space and second or higher order in time. Then we consider some peculiarities of implementation of the derived finite difference schemes.

6.1 Case $\alpha_R = 0$ or $\alpha_L = 0$

This extreme case corresponds to the familiar Variance Gamma model. In this case the integrals in Eqs. 62 and 68 exist if we keep just first two terms under the integral. Therefore we could integrate out the last term $R \propto \frac{\partial}{\partial x} C(x, \tau)(e^y - 1)$. This term then will become a part of the convection part of the total PIDE and therefore we will not

[6] A second order approximation could in principle be constructed as well, however resulting in a massive calculation of the coefficients. That probably stopped the scientists to further elaborate this approach.

[7] In principal one can eliminate special cases when one of the following conditions is valid $\alpha_R = 0, \alpha_L = 0, \alpha_R = 1, \alpha_L = 1$, by just substituting, say $\alpha_R = \epsilon \ll 1$ instead of $\alpha_R = 0, \alpha_R = 1 + \epsilon$ instead of $\alpha_R = 1$, etc.

consider it here, assuming that we use a splitting technique and know how to solve the remaining convection-diffusion equation.

Then Eq. 63 could be written in the form of Eq. 39 with

$$\begin{aligned} \mathcal{B}_R &= \sqrt{V_R}\lambda_R \left\{ \log(\nu_R) - \log\left(\nu_R - \frac{\partial}{\partial x}\right)\right\} \\ \mathcal{B}_L &= \sqrt{V_L}\lambda_L \left\{ \log(\nu_L) - \log\left(\nu_L + \frac{\partial}{\partial x}\right)\right\} \end{aligned} \tag{75}$$

Therefore, integrating it we obtain an explicit form of Eq. 42

$$\begin{aligned} C^{k+1}(x) &= \left(1 - \frac{1}{\nu_R}\frac{\partial}{\partial x}\right)^{-m} C^k(x), \quad m = \sqrt{V_R}\lambda_R\theta > 0, \\ C^{k+1}(x) &= \left(1 + \frac{1}{\nu_L}\frac{\partial}{\partial x}\right)^{-m} C^k(x), \quad m = \sqrt{V_L}\lambda_L\theta, \end{aligned} \tag{76}$$

In practical computation of the rhs operators we exploit a modification of our interpolation method which was described above. First, note that typical values of λ_R, λ_L as well as V_R, V_L are limited, i.e. normally $\lambda_R < M, \lambda_L < M, V_R < M, V_L < M$ where M could be chosen in the range, say 3–5. Second, if we solve a general jump-diffusion equation using some kind of splitting methods, the time step of integration θ in Eq. 76 is determined by the time step used at the integration of the diffusion part. This means that θ is usually small. Therefore, it is pretty reasonable to assume that in Eq. 76 $m < 2$. Next, as follows from the definition of the fractional derivatives, the operators in Eq. 76 are continuous in m. Therefore, we could solve Eq. 76 for $m = 0, 1, 2$ and then use quadratic interpolation to get the solution given the real value of m, and the condition $m < 2$. Note, that $m = 0$ is a trivial case so the solution $C^{k+1}(X) = C^k(x)$ is already known.

Note a choice of $m = -1$. On the one hand this is very attractive because then the solution of Eq. 76 is already found. On the other hand at $m < 0$ the scheme in Eq. 76 becomes explicit which breaks its unconditional stability. Apparently the best one can achieve in this case is to use a central difference approximation for the first derivative. Then it is possible to show that all eigenvalues of the rhs matrix have their real value equal to one. Thus the stability of the scheme is questionable.

We now construct a stable FD scheme to solve the first equation in Eq. 76. Similar to what was already discussed in the previous section a forward second order approximation of the first derivative has to be chosen. Then the eigenvalues of the discrete operator $\left(1 - \frac{1}{\nu_R}\frac{\Delta}{\Delta x}\right)^{-m}$ are

$$\zeta = \left(1 + \frac{3}{2h\nu_R}\right)^{-m}. \tag{77}$$

We need to guarantee that $\| \left(1 - \frac{1}{\nu_R}\frac{\Delta}{\Delta x}\right)^{-m} \| < 1$. Thus, if $\nu_R < 1$ this FD scheme is stable at $h < 3/[2(1-\nu_R)]$, and if $\nu_R \geq 1$—it is unconditionally stable. As follows from the Proposition Eq. 7 $\mathbb{R}(\nu_R) > 1$, therefore the scheme is unconditionally stable.

After this discretization the matrix of the lhs operator becomes one-sided tridiagonal if $m = 1$, and one-sided pentadiagonal if $m = 2$. Therefore this equation can be efficiently solved with the total complexity $O(N(2m+1))$.

To preserve monotonicity of the solution for the second equation in Eq. 76 a backward second order approximation of the first derivative has to be chosen. This approximation was also already introduced in the previous section. Then $C^{k+1}(x,m)$ can be computed as a product $A_m \cdot C^k(x)$, where A_m is a band matrix with $2m+1$ diagonals. So the complexity of this is also $O(N(2m+1))$.

Based on these results we extend our numerical test described in the previous section to the case $\alpha_R = 0$. However, to preserve convergence of the integral now instead of Eq. 59 we have to use the extended equation

$$\frac{\partial}{\partial \tau} C(x,\tau) = \int_0^\infty [C(x+y,\tau) - C(x,\tau)]\, \lambda_R \frac{e^{-\nu_R |y|}}{|y|^{1+\alpha_R}} dy, \quad \alpha_R < -1 \tag{78}$$

We again compare the FFT solution of Eq. 78 with that obtained based on our method.

FFT It should be underlined that the presented simple FFT algorithm completely loses its accuracy when $\alpha_R \to 0$. Therefore, instead of $\alpha_R = 0$ we will chose real $\alpha_R = -0.5$. We again define a uniform grid in the domain $(-x_*, x_*)$ which contains N points: $x_1 = -x_*, x_2, \ldots, x_{N-1}, x_N = x_*$ such that $x_i - x_{i-1} = h, i = 2 \ldots N$. We then approximate the integral in the rhs of Eq. 78 with the first order of accuracy in h as

$$\begin{aligned} &\int_0^\infty [C(x+y,\tau) - C(x,\tau)]\, \lambda_R \frac{e^{-\nu_R |y|}}{|y|^{1+\alpha_R}} dy \\ &= h \sum_{j=1-i}^{N-i} C_{i+j}(\tau) f_j - C(x,\tau) \lambda_R \nu_R^{\alpha_R} \Gamma(-\alpha_R), \\ &f_j \equiv \lambda_R \frac{e^{-\nu_R |x_j|}}{|x_j|^{1+\alpha_R}} + O(h^2) \end{aligned} \tag{79}$$

The matrix-vector product in the lhs of Eq. 79 is computed using FFT as it was described in the previous section.

FD We solve Eq. 78 using interpolation in α_R between the points $\alpha_R = 0, -1, -2, -3$. At $\alpha_R = 0$ we use the FD scheme in Eq. 76. At $\alpha_R < 0$ we again use our

approach of construction of the pseudo-parabolic equations (see Propositions 3, 4), and instead of Eq. 39 now obtain

$$\frac{\partial}{\partial\tau}C(x,t)=\mathcal{B}C(x,t),\quad \mathcal{B}\equiv\frac{1}{2}(\mathcal{A}_x^-)^{-1}-\lambda_R\nu_R^{\alpha_R}\Gamma(-\alpha_R). \tag{80}$$

Further we use the Crank-Nicolson scheme Eq. 44 which now reads

$$\begin{aligned}&\left(\left[1+\frac{1}{2}\lambda_R\nu_R^{\alpha_R}\Gamma(-\alpha_R)\theta\right]\mathcal{A}_x^- -\frac{1}{4}\theta\right)C^{k+1}(x)\\&\quad=\left(\left[1-\frac{1}{2}\lambda_R\nu_R^{\alpha_R}\Gamma(-\alpha_R)\theta\right]\mathcal{A}_x^- +\frac{1}{4}\theta\right)C^{k}(x).\end{aligned} \tag{81}$$

The stability analysis could be provided similar to what we did in the previous sections. Again it is easy to show that the forward one-sided approximation of the operator $\mathcal{A}_x^-$ given in Eq. 51 guarantees the unconditional stability of the above scheme.

Comparison The results of this test are very close to that given in Fig. 1. The difference is that the results presented in the Fig. 1 could be extended to $\alpha=0$ by computing the option prices at $\alpha=-3,-2,-1$ and then using extrapolation. Here instead of extrapolation we use interpolation, because we are able to solve our test problem numerically at $\alpha_R=0$. Surprisingly the difference in the FFT and FD solutions very slightly increases in case of interpolation. The FD solution is still faster than the FFT (about 2.5 times slower than the results presented in Table 3), and as follows from the above analysis—more accurate.

6.2 Case $\alpha_R=1,\alpha_L=1$

This is a case of jumps with infinite variation and infinite activity. Therefore we have to keep the whole integrals in Eqs. 62 and 68, i.e. in each integral we can not integrate the last term out because otherwise the integral does not converge.

Let us remind that as follows from the Proposition 7 in this case the original PIDE Eq. 62 is equivalent to the PIDE

$$\begin{aligned}\frac{\partial}{\partial\tau}C(x,V_R,V_L,\tau)&=\sqrt{V_R}\lambda_R\left\{-\nu_R\log\nu_R+(\nu_R-\frac{\partial}{\partial x})\log\left(\nu_R-\frac{\partial}{\partial x}\right)\right.\\&\left.+\left[\nu_R\log\nu_R-(\nu_R-1)\log(\nu_R-1)\right]\frac{\partial}{\partial x}\right\}C(x,V_R,V_L,\tau)\\&\mathbb{R}(\partial/\partial x)<0,\mathbb{R}(\nu_R)>1,\end{aligned} \tag{82}$$

while from Proposition 8 the PIDE Eq. 71 is equivalent to the PIDE

$$\frac{\partial}{\partial\tau}C(x,V_R,V_L,\tau)=\sqrt{V_L}\lambda_L\left\{-\nu_L\log\nu_L\right.$$

$$+\left[\nu_L \log \nu_L - (\nu_L+1)\log(\nu_L+1)\right]\frac{\partial}{\partial x} + (\nu_L + \frac{\partial}{\partial x})\log\left(\nu_L + \frac{\partial}{\partial x}\right)\Big\}$$
$$C(x, V_R, V_L, \tau)\ \mathbb{R}(\partial/\partial x) < 0, \quad \mathbb{R}(\nu_L) > 0. \tag{83}$$

For the following we need to prove the following proposition.

Proposition 9 *The following identity holds*

$$-\nu_R \log \nu_R + (\nu_R - \frac{\partial}{\partial x})\log\left(\nu_R - \frac{\partial}{\partial x}\right) + \left[\nu_R \log \nu_R - (\nu_R - 1)\log(\nu_R - 1)\right]\frac{\partial}{\partial x}$$
$$= \int_\nu^\infty \left\{\log \nu_R - \log\left(\nu_R - \frac{\partial}{\partial x}\right) + \left(\log\frac{\nu_R - 1}{\nu_R}\right)\frac{\partial}{\partial x}\right\} d\nu \tag{84}$$

Proof To prove this we have to note that

$$\int_\nu^\infty \frac{e^{-\nu_R|y|}}{|y|^{1+\alpha_R}} d\nu = \frac{e^{-\nu_R|y|}}{|y|^{2+\alpha_R}}, \tag{85}$$

and then use Proposition 7 with $\alpha_R = 0$. □

In a similar way we can prove the following proposition

Proposition 10

$$-\nu_L \log \nu_L + \left[\nu_L \log \nu_L - (\nu_L+1)\log(\nu_L+1)\right]\frac{\partial}{\partial x} + (\nu_L + \frac{\partial}{\partial x})\log\left(\nu_L + \frac{\partial}{\partial x}\right)$$
$$= \int_\nu^\infty \left\{\log(\nu_L) - \log\left(\nu_L + \frac{\partial}{\partial x}\right) + \log\left(\frac{\nu_L + 1}{\nu_L}\right)\frac{\partial}{\partial x}\right\} d\nu \tag{86}$$

These two identities gives us an idea of how to construct a FD numerical method for solving Eqs. 82 and 83. First we rewrite Eqs. 82 and 83 in the form

$$\frac{\partial}{\partial \tau} C(x, V_R, V_L, \tau) = \mathbb{L}_R C(x, V_R, V_L, \tau) \tag{87}$$
$$\frac{\partial}{\partial \tau} C(x, V_R, V_L, \tau) = \mathbb{L}_L C(x, V_R, V_L, \tau)$$
$$\mathbb{L}_R \equiv \sqrt{V_R}\lambda_R \int_\nu^\infty \left\{\log(\nu_R) - \log\left(\nu_R - \frac{\partial}{\partial x}\right) + \left(\log\frac{\nu_R - 1}{\nu_R}\right)\frac{\partial}{\partial x}\right\} d\nu$$
$$\mathbb{L}_L \equiv \sqrt{V_L}\lambda_L \int_\nu^\infty \left\{\log(\nu_L) - \log\left(\nu_L + \frac{\partial}{\partial x}\right) + \log\left(\frac{\nu_L + 1}{\nu_L}\right)\frac{\partial}{\partial x}\right\} d\nu$$

We already know how to solve these equations if the operators $\mathbb{L}_R$ and $\mathbb{L}_L$ do not contain the integrals. We want to utilize this approach by proceeding with the following steps.

Step 1 First we truncate the upper limit in the integral to some ν_*. This could be done because the integral in Eq. 87 is well-defined and at $\nu_R \to \infty$ the integral kernel tends to zero as

$$\lim_{\nu_R \to \infty} \mathbb{L}_R C(x, V_R, V_L, \tau) = \sqrt{V_R}\lambda_R \frac{1}{2\nu_R^2}\left(-\frac{\partial}{\partial x} + \frac{\partial^2}{\partial x^2}\right) + O\left(1/\nu_R^3\right) \quad (88)$$

At the interval (ν, ν_*) we approximate the integral in ν using some quadrature formula, for instance, the well-known Simpson formula (higher-order approximations of even adaptive quadratures could definitely be used as well). So we partition the interval (ν, ν_*) into an even number of intervals M all of the same width $h = (\nu_* - \nu)/M$. Then operators in Eq. 87 transform to

$$\begin{aligned}
\mathbb{L}_R &\equiv \sum_{i=0}^{M} \mathbb{L}_{i,R}, \quad \mathbb{L}_L \equiv \sum_{i=0}^{M} \mathbb{L}_{i,L} \\
\mathbb{L}_{i,R} &= a_i \sqrt{V_R}\lambda_R \frac{\nu_* - \nu}{3M}\left\{\log(\nu_{i,R}) - \log\left(\nu_{i,R} - \frac{\partial}{\partial x}\right) + \left(\log\frac{\nu_{i,R} - 1}{\nu_{i,R}}\right)\frac{\partial}{\partial x}\right\} \\
\mathbb{L}_{i,L} &\equiv a_i \sqrt{V_L}\lambda_L \frac{\nu_* - \nu}{3M}\left\{\log(\nu_{i,L}) - \log\left(\nu_{i,L} + \frac{\partial}{\partial x}\right) + \log\left(\frac{\nu_{i,L} + 1}{\nu_{i,L}}\right)\frac{\partial}{\partial x}\right\}, \\
a_i &= 1, \quad i = 0, M, \; a_i = 2, \quad i = 2, 4 \ldots M - 2, \; a_i = 4, \quad i = 1, 3 \ldots M - 1.
\end{aligned} \quad (89)$$

Step 2 Each operator in Eq. 89 is a sum of M operators which commute with each other. Therefore, the solution of Eq. 87 reads

$$\begin{aligned}
C(x, V_R, V_L, \tau) &= \exp\left[\sum_{i=0}^{M} \mathbb{L}_{i,R}\tau\right] C(x, V_R, V_L, 0) = \prod_{i=1}^{M} e^{\mathbb{L}_{i,R}\tau} C(x, V_R, V_L, 0) \\
C(x, V_R, V_L, \tau) &= \exp\left[\sum_{i=0}^{M} \mathbb{L}_{i,L}\tau\right] C(x, V_R, V_L, 0) = \prod_{i=1}^{M} e^{\mathbb{L}_{i,L}\tau} C(x, V_R, V_L, 0)
\end{aligned} \quad (90)$$

Using a splitting technique (see, for instance, Lanser and Verwer 1999; Yoshida 1990) we can represent this equation in the form

$$\begin{aligned} C_1(x,V_R,V_L,\theta) &= e^{\mathbb{L}_{1,R}\tau}C(x,V_R,V_L,0)\\ C_2(x,V_R,V_L,\theta) &= e^{\mathbb{L}_{2,R}\tau}C_1(x,V_R,V_L,\theta)\\ &\cdots\cdots\cdots\cdots\cdots\cdots\cdots\cdots\\ C_M(x,V_R,V_L,\theta) &= e^{\mathbb{L}_{M,R}\tau}C_{M-1}(x,V_R,V_L,\theta)\\ C(x,V_R,V_L,\theta) &= C_M(x,V_R,V_L,\theta) \end{aligned} \tag{91}$$

and similarly for the operator $\mathbb{L}_L$.

Step 3 Each equation in Eq. 91 is very similar to that corresponding to the case $\alpha = 0$ (see the previous section).The only difference is that the operators $\mathbb{L}_{i,R}$ now contain an extra term $\mathbb{L}_{3,i,R} = \left(\log\frac{\nu_{i,R}-1}{\nu_{i,R}}\right)\frac{\partial}{\partial x}$, and the operators $\mathbb{L}_{i,L}$ now contain an extra term $\mathbb{L}_{3,i,L} = \left(\log\frac{\nu_{i,L}+1}{\nu_{i,L}}\right)\frac{\partial}{\partial x}$. We can apply splitting to these operators similar to as we did in the above. Further by analogy with what was already discussed in the previous sections devoted to Páde approximations, these terms $e^{\mathbb{L}_{3,i,R}\theta}$ and $e^{\mathbb{L}_{3,i,L}\theta}$ could be approximated with the second order of accuracy in θ by using Eq. 43. Finally, each equation in Eq. 91 reads

$$\begin{aligned} &C_{-1}^{k+1}(x) = C^k(x)\\ &\begin{cases} C_{i*}^{k+1}(x) = \dfrac{1+\frac{m_i}{2}\mathbb{L}_{3,i,R}}{1-\frac{m_i}{2}\mathbb{L}_{3,i,R}}C_{i-1}^{k}(x)\\ C_{i}^{k+1}(x) = \left(1-\dfrac{1}{\nu_{1,R}}\dfrac{\partial}{\partial x}\right)^{-m_i}C_{i*}^{k}(x) \end{cases} \qquad i=0,\dots,M,\quad m_i \equiv a_i\theta\sqrt{V_R}\lambda_R\frac{\nu_*-\nu}{3M}\\ &C^{k+1}(x) = C_M^{k+1}(x) \end{aligned} \tag{92}$$

We can choose the number M to guarantee that the value of m_i is less than 2 and then use interpolation solving the above equations at $m_i = 0, 1, 2$.

Similar scheme could be constructed for the operator $\mathbb{L}_L$, which reads

$$\begin{aligned} &C_{-1}^{k+1}(x) = C^k(x)\\ &\begin{cases} C_{i*}^{k+1}(x) = \dfrac{1+\frac{m_i}{2}\mathbb{L}_{3,i,L}}{1-\frac{m_i}{2}\mathbb{L}_{3,i,L}}C_{i-1}^{k+1}(x)\\ C_{i}^{k+1}(x) = \left(1+\dfrac{1}{\nu_{i,L}}\dfrac{\partial}{\partial x}\right)^{-m_i}C_{i*}^{k+1}(x) \end{cases} \qquad i=0,\dots,M,\quad m_i \equiv a_i\theta\sqrt{V_L}\lambda_L\frac{\nu_*-\nu}{3M}\\ &C^{k+1}(x) = C_M^{k+1}(x) \end{aligned} \tag{93}$$

Step 4 To construct an unconditionally stable scheme in x we have to choose approximation for the first derivative in Eq. 92. If we rewrite this equation in the form

$$
\begin{aligned}
C_{-1}^{k+1}(x) &= C^k(x) \\
\left[1-\frac{m_i\theta}{2}\left(\log\frac{\nu_{i,R}-1}{\nu_{i,R}}\right)\frac{\partial}{\partial x}\right]C_{i*}^{k+1}(x) &= \left[1+\frac{m_i\theta}{2}\left(\log\frac{\nu_{i,R}-1}{\nu_{i,R}}\right)\frac{\partial}{\partial x}\right]C_{i-1}^{k}(x), \quad i=0,\ldots,M \\
\left(1-\frac{1}{\nu_{i,R}}\frac{\partial}{\partial x}\right)^{m_i} C_i^k(x) &= C_{i*}^k(x) \\
C^{k+1}(x) &= C_M^{k+1}(x)
\end{aligned}
\tag{94}
$$

it becomes obvious that the derivative in the second equation in Eq. 94 should be approximated by using a backward one-sided second order divided difference. For the derivative in the third equation one has to use a forward approximation.

Similarly we rewrite Eq. 93 in the form

$$
\begin{aligned}
C_{-1}^{k+1}(x) &= C^k(x) \\
\left[1-\frac{m_i\theta}{2}\left(\log\frac{\nu_{i,L}+1}{\nu_{i,L}}\right)\frac{\partial}{\partial x}\right]C_{i*}^{k+1}(x) &= \left[1+\frac{m_i\theta}{2}\left(\log\frac{\nu_{i,L}+1}{\nu_{i,L}}\right)\frac{\partial}{\partial x}\right]C_{i-1}^{k}(x), \\
& \qquad i=0,\ldots,M \\
\left(1+\frac{1}{\nu_{i,L}}\frac{\partial}{\partial x}\right)^{m_i} C_i^{k+1}(x) &= C_{i*}^k(x) \\
C^{k+1}(x) &= C_M^{k+1}(x)
\end{aligned}
\tag{95}
$$

and use a forward approximation for the derivative in the second equation in Eq. 95 and the backward approximation in the third equation.

The matrix in the rhs of the second equation in the Eq. 95 is upper tridiagonal. The matrix in the rhs of the third equation in the Eq. 95 is lower tridiagonal at $m_i = 1$ and lower pentadiagonal at $m_i = 2$. The total complexity of the algorithm as compared with the case $\alpha = 0$ is: one extra equation at each step, M steps instead of just one in the case $\alpha = 0$. Therefore, using the results obtained for $\alpha = 0$ (see Table 3 and remember, that for $\alpha = 0$ the performance of our algorithm is about 2.5 times slower) we can expect that at $M = 30$ this algorithm is about 3 times slower than the FFT. On the other hand it provides the second order approximation in both space and time, and does not require to re-interpolate the FFT results to the FD grid which was previously used to find solution for the diffusion part of the original PIDE.

To verify this we provided two numerical experiments. In the first experiment ν_* varied while $h = (\nu_* - \nu_R)/M$ was chosen to be constant. At $\nu_* = 5$ we choose $M = 30$. The other parameters are same as in the previous numerical experiments reported in the above. This results are presented in Fig. 7.

The computational time rawly increases by the factor $M/2$, i.e. for $M = 30$ it is almost same as for the corresponding FFT. It is seen that if $x < 3$ small ν_* provide a good accuracy of computation, while at $3 < x < 5$ an appropriate value of ν_* should be more than 300.

In the second experiment we fixed the value $\nu_* = 300$ and varied M to see at which M one could expect to get convergency. These results are presented in Fig 8. As it is seen $M = 80$ seems to be sufficient to obtain the convergency. The computational

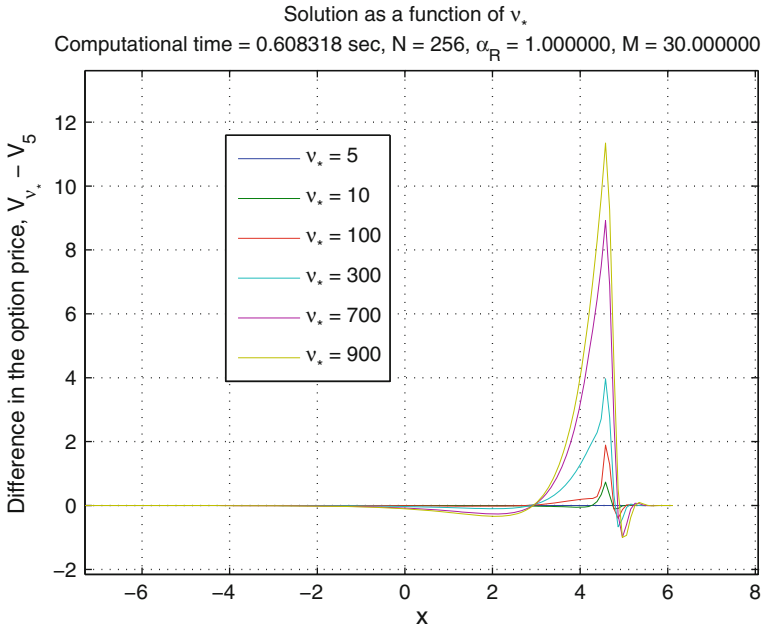

Fig. 7 Difference in solutions of Eq. 94 obtained at various ν_* and that at $\nu_* = 5$ at $M = 30$ and $\alpha_R = 1$

time in the case $M = 81$ is 1.4 s which is 3.6 times more than that for the FFT. Thus, in this case our algorithm is almost 4 times slower than the FFT. As it was already mentioned this could be compensated (a) by the second order of accuracy in space and time, and (b) no need for re-interpolation of the FFT results to the FD grid. One more advantage is that we don't need to treat the point $y = 0$ in a special way as it was done, say in Cont and Voltchkova (2003).

Note, that as we use M steps in the splitting scheme, the error in time becomes $O(M\theta^2)$ that could kill the second order of approximation. Therefore, for instance, in Eq. 92 it is better to use a third order approximation in time (see Eq. 46). Accordingly the second equation in Eq. 94 will become

$$\left[1 - \frac{2p_i\theta}{3} + \frac{p_i^2\theta^2}{6}\right] C_{i*}^{k+1}(x) = \left[1 + \frac{p_i\theta}{3}\right] C_{i-1}^{k}(x)$$

$$p_i = m_i \left(\log \frac{\nu_{i,R} - 1}{\nu_{i,R}}\right) \frac{\partial}{\partial x}, \quad i = 0, \ldots, M \tag{96}$$

To preserve the third order of approximation in time the third equation in Eq. 94 should now be solved at $m = 0, 1, 2, 3$ and then cubic interpolation to the actual value m_i will give the final solution. This scheme increases the total computational time by about 10%, however the accuracy in time increases to $O(M\theta^3)$.

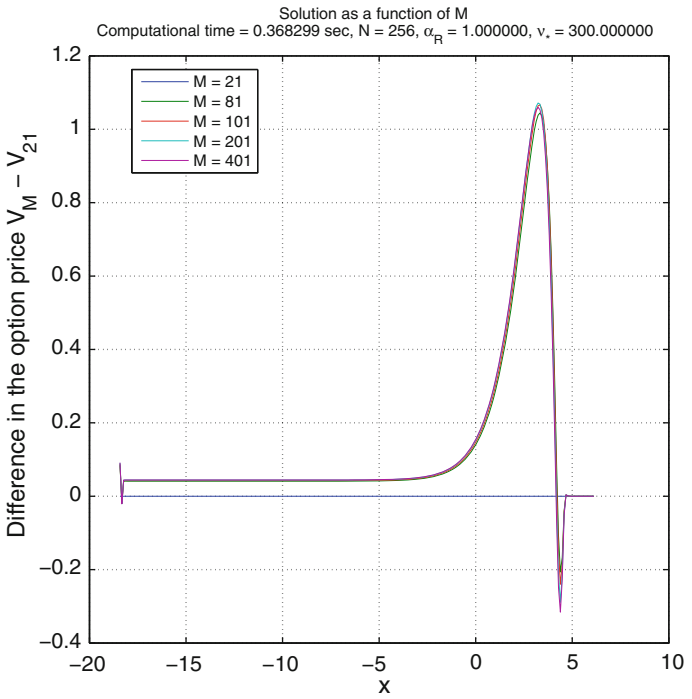

Fig. 8 Difference in solutions of Eq. 94 obtained at various M and that at $M = 21$ at $\nu_* = 300$ and $\alpha_R = 1$

7 Conclusion

From the numerical point of view our approach has some advantages as compared with the methods reviewed in Sect. 1. Indeed, first we managed to reduce the original evolutionary integral equation to the pure differential equation. Second, this equation could be formally solved analytically. Then to compute the operator exponent we applied a Padé approximation technique and derived finite difference equations which approximate the original solution with the necessary order of accuracy. These equations could be solved at the same grid as the diffusion part of the original PIDE, thus eliminating problems inherent to the FFT methods. Next, despite the original integral term is non-local, the matrix $\mathcal{D}$ of the system of linear equations (which were obtained by the direct application of our method) is the band matrix in case of the integer $\alpha_{R,L}$. In other words, it corresponds to a local approximation of the option price, which is definitely a plus for the numerical algorithm. Also we demonstrated that at $\alpha \leq 0$ the complexity of our algorithm is much lower (almost 30 times faster than that of the FFT), while the accuracy is much better (for practical purpose we can use the second or third order FD approximation whereas getting same approximation within the FFT method will significantly increase the complexity).

The complexity of our solution at $\alpha = 1$ is almost 4 times higher than that of the FFT. This in part is compensated by few factors: (i) our algorithm provides the second

order approximation in both space and time, and (ii) it does not require to re-interpolate the FFT results to the FD grid which was previously used to find the solution for the diffusion part of the original PIDE.

Using this technique the solution at $2 > \alpha > 1$ could be obtained by using extrapolation given the solution at $\alpha = 1, 0, -1$.

It is interesting to know what are real values of α. In Bu (2007) the author used to calibrate the CGMY model to S&P 500 historical call option prices. The market prices were chosen from June 2007 to December 2008. The strikes were from 1300 to 2000 and collected into two groups: with the increment of 25 from 1300 to 1700, and with the increment of 100 from 1700 to 2000. The index closed price is 1536.34. Thus found the CGMY parameters were: $C = 0.0156$, $G = 0.0767$, $M = 7.5500$, $Y = 1.2996$, i.e. in our notation $\alpha = Y = 1.3$. In Carr et al. (2005) the option prices of S&P 500 were also calibrated using the CGMY model which gave the values of α in the range $(-0.39, -0.42)$. Therefore, our results could be useful in pricing real options at both positive and negative values of α.

Appendix 1

Here we prove the following propositions.

Proposition 5 *Both integrals in Eq. 21 are continuous in α at $\alpha < 2$.*

Proof To prove this we use a series representation of the integrals in variable y

$$
\begin{aligned}
I_L &= \sqrt{V_L}\int\limits_{-\infty}^{0}\left[C(x+y,\Omega,\tau) - C(x,\Omega,\tau) - \frac{\partial}{\partial x}C(x,\Omega,\tau)y\right]\lambda\frac{e^{-|y|\nu}}{|y|^{1+\alpha}}dy \\
&= \sqrt{V_L}\sum_{n=2}^{\infty} a_n \frac{\partial^n}{\partial x^n}C(x,\Omega,\tau), \\
I_R &= \sqrt{V_R}\int\limits_{0}^{\infty}\left[C(x+y,\Omega,\tau) - C(x,\Omega,\tau) - \frac{\partial}{\partial x}C(x,\Omega,\tau)y\right]\lambda\frac{e^{-|y|\nu}}{|y|^{1+\alpha}}dy \\
&= \sqrt{V_R}\sum_{n=2}^{\infty} b_n \frac{\partial^n}{\partial x^n}C(x,\Omega,\tau), \\
a_n &= \int\limits_{-\infty}^{0}\frac{y^{n+1}}{n!}\lambda\frac{e^{-|y|\nu}}{|y|^{1+\alpha}}dy, \quad b_n = \int\limits_{0}^{\infty}\frac{y^{n+1}}{n!}\lambda\frac{e^{-|y|\nu}}{|y|^{1+\alpha}}dy.
\end{aligned}
\tag{97}
$$

Then at $\alpha < 2$ coefficients a_n and b_n, $n \geq 2$ are regular functions of α. So the integrand kernels in the definition of a_n, b_n are continuous functions of α as well as a_n and b_n. □

Proposition 6 *Assume that in Eq. 27* $\alpha \in \mathbb{R}, \alpha \leq -1$. *Then the solution of Eq. 27 with respect to* $\mathcal{A}_x^+$ *is*

$$\mathcal{A}_x^+ = \frac{1}{\lambda\Gamma(p+1)}\left(\nu + \frac{\partial}{\partial x}\right)^{p+1} \equiv \frac{1}{\lambda\Gamma(p+1)}\left[\sum_{i=0}^{\infty} C_i^{p+1}\nu^{p+1-i}\frac{\partial^i}{\partial x^i}\right],$$
$$p \equiv -(1+\alpha) \geq 0,$$

where C_i^{p+1} *are the generalized binomial coefficients which could be expressed via Gamma function, and fractional derivatives are understood in the Riemann-Liouville sense (Oldham and Spanier 1974).*

Proof Taking Laplace Transform of the expression $\mathcal{A}^+ f(x)$ we obtain

$$\begin{aligned}\mathcal{L}_s\left(\mathcal{A}_x^+ f(x)\right) &= \mathcal{L}_s\left\{\frac{1}{\lambda\Gamma(p+1)}\left[\sum_{i=0}^{\infty} C_i^{p+1}\nu^{p+1-i}\frac{\partial^i}{\partial x^i}\right] f(x)\right\} \\ &= \frac{1}{\lambda\Gamma(p+1)}\left[\sum_{i=0}^{\infty} C_i^{p+1}\nu^{p+1-i}s^i\right]\mathcal{L}_s f(x) \\ &= \frac{1}{\lambda\Gamma(p+1)}(\nu+s)^{p+1}\mathcal{L}_s f(x)\end{aligned}$$

Now, as

$$f(x) = \lambda\frac{e^{-\nu|x|}}{|x|^{1+\alpha}}\mathbf{1}_{y>0}$$

and

$$\mathcal{L}_s\left\{\lambda\frac{e^{-\nu|x|}}{|x|^{1+\alpha}}\mathbf{1}_{x>0}\right\} = \lambda\Gamma(p+1)(\nu+s)^{-(1+p)},$$

we obtain

$$\mathcal{L}_s\left(\mathcal{A}_x^+ f(x)\right) = 1 = \mathcal{L}_s\delta(x)$$

And thus $\mathcal{A}_x^+ f(x) = \delta(x)$ □

Another proof is based on a different idea.

Proof As it is well known a shift operator in L2 space could be represented as follows

$$\mathfrak{S}_a = \exp\left(a\frac{\partial}{\partial x}\right), \tag{98}$$

so

$$\mathfrak{S}_a f(x) = f(x+a).$$

Therefore, the integrals in Eq. 24 could be formally rewritten as

$$\mathcal{A}_1 C(x,t), \mathcal{A}_1 \equiv \int_0^\infty \lambda_R \frac{e^{-\nu_R|y|}}{|y|^{1+\alpha_R}} \exp\left(y\frac{\partial}{\partial x}\right) dy$$
$$\mathcal{A}_2 C(x,t), \mathcal{A}_2 \equiv \int_{-\infty}^0 \lambda_L \frac{e^{-\nu_L|y|}}{|y|^{1+\alpha_L}} \exp\left(y\frac{\partial}{\partial x}\right) dy \tag{99}$$

We can compute these integrals assuming that $\partial/\partial x$ is a constant. This gives

$$\mathcal{A}_1 = \lambda_R \Gamma(-\alpha_R)\left(\nu_R - \frac{\partial}{\partial x}\right)^{\alpha_R}, \quad \mathbb{R}(\alpha) < 0, \mathbb{R}(\nu_R - \partial/\partial x) > 0$$
$$\mathcal{A}_2 = \lambda_L \Gamma(-\alpha_L)\left(\nu_L + \frac{\partial}{\partial x}\right)^{\alpha_L}, \quad \mathbb{R}(\alpha) < 0, \mathbb{R}(\nu_L + \partial/\partial x) > 0, \tag{100}$$

where under a real part of differential operator we will understand the real part of the maximum eigenvalue of finite difference matrix which approximates this differential operator (see below).

A simple observation shows that

$$\mathcal{A}_1 = \left(\mathcal{A}_x^-\right)^{-1}, \quad \mathcal{A}_2 = \left(\mathcal{A}_x^+\right)^{-1},$$

which finalizes the proof. □

Acknowledgments We thank Alex Lipton, participants of Global Derivatives & Risk Conference, 2010 and the 6th Bachelier Congress, 2010 as well as two anonymous referees for their useful comments.

References

Abu-Saman, A. M., & Assaf, A. M. (2007). Stability and convergence of Crank-Nicholson method for fractional advection dispersion equation. *Advances in Applied Mathematical Analysis, 2*, 117–125.

Amin, K. (1993). Jump diffusion option valuation in discrete time. *Journal of Finance, 48*, 1833–1863.

Andersen, L., & Andreasen, J. (2000). Jump diffusion processes: Volatility smile fitting and numerical methods for option pricing. *Review of Derivatives Research, 4*, 231–262.

Bakas, I., Khesin, B., & Kiritsis, E. (1993). The logarithm of the derivative operator and higher spin algebras of w_∞ type. *Communications in Mathematical Physics, 151*(2), 233–243.

Boyarchenko, S., & Levendorskii, S. (2002). *Non-Gaussian Merton–Black–Scholes theory*. Singapore: World Scientific.

Bu, Y. (2007). *Option pricing using Levy processes*. PhD thesis, Department of Mathematical Statistics, Chalmers University of Technology and Goteborg University, GA.

Cannon, J., & Lin, Y. (1988). Classical and weak solutions for one-dimensional pseudo-parabolic equations with typical boundary data. *Annali di Matematica Pura Ed Applicata, 152*, 375–385.

Carr, P., Geman, H., Madan, D., & Yor, M. (2002). The fine structure of asset returns: An empirical investigation. *Journal of Business, 75*, 305–332.

Carr, P., Geman, G., Madan, D., & Yor, M. (2005). Pricing options on realized variance. *Finance and Stochastics, 4*, 453–475.

Carr, P., & Mayo, A. (2007). On the numerical evaluation of option prices in jump diffusion processes. *The European Journal of Finance, 13*, 353–372.

Carr, P., & Wux, L. (2004). Time-changed Lévy processes and option pricing. *Journal of Financial Economics, 71*, 113–141.
Cartea, A., & del Castillo-Negrete, D. (2007). Fractional diffusion models of option prices in markets with jumps. *Physica A, 374*, 749–763.
Cont, R. (Ed.). (2009). *Frontiers in quantitative finance: Volatility and credit risk modeling*. New York: Wiley Finance Press.
Cont, R., & Tankov, P. (2004). *Financial modelling with jump processes. Financial matematics series*. Boca Raton: Chapman & Hall/CRC.
Cont, R., & Voltchkova, E. (2003). A finite difference scheme for option pricing in jump diffusion and exponential Lévy models. Technical Report 513, Rapport Interne CMAP.
d'Halluin, Y., Forsyth, P. A., & Labahn, G. (2005). A semi-lagrangian approach for American Asian options under jump diffusion. *SIAM Journal on Scientific Computing, 27*, 315–345.
d'Halluin, Y., Forsyth, P. A., & Vetzal, K. R. (2004). A penalty method for American options with jump diffusion processes. *Numerische Mathematik, 97*, 321–352.
d'Halluin, Y., Forsyth, P. A., & Vetzal, K. R. (2005). Robust numerical methods for contingent claims under jump diffusion processes. *IMA Journal of Numerical Analysis, 25*, 87–112.
Eberly, D. (2008). Derivative approximation by finite differences. http://www.geometrictools.com/Documentation/FiniteDifferences.pdf. Accessed 2 March 2008.
Evans, M., Hastings, N., & Peacock, B. (2000). Erlang distribution. In *Statistical distributions* (3rd ed., Chap. 12, pp. 71–73). New York: Wiley.
Hilber, N., Reich, N., Schwab, C., & Winter, C. (2009). Numerical methods for Lévy processes. *Finance and Stochastics, 13*, 471–500.
In't Hout, K. J., & Welfert, B. D. (2009). Unconditional stability of second-order ADI schemes applied to multi-dimensional diffusion equations with mixed derivative terms. *Applied Numerical Mathematics, 59*, 677–692.
Itkin, A., & Carr, P. (2006). Finite-difference approach to pricing barrier options under stochastic skew model. In *Global derivatives & risk conference, May 8–12, Paris, France*. http://www.chem.ucla.edu/~itkin/publications/Paris2006.pdf.
Itkin, A., & Carr, P. (2011). Jumps without tears: A new splitting technology for barrier options. *IJNAM, 8*(4), 667–704.
Koponen, I. (1995). Analytic approach to the problem of convergence of truncated Levy flights towards the gaussian stochastic process. *Physical Review E, 52*, 1197–1199.
Lanser, D., & Verwer, J. (1999). Analysis of operator splitting for advection–discussion–reaction problems from air pollution modelling. *Journal of Computational and Applied Mathematics, 111*, 201–216.
Lipton, A., & Sepp, A. (2009). Credit value adjustment for credit default swaps via the structural default model. *The Journal of Credit Risk, 5*, 123–146.
Madan, D., & Seneta, E. (1990). The variance gamma (V.G.) model for share market returns. *Journal of Business, 63*, 511–524.
Marom, O., & Momoniat, E. (2009). A comparison of numerical solutions of fractional diffusion models in finance. *Nonlinear Analysis: Real World Applications, 10*, 3435–3442.
Matache, A., von Petersdorff, T., & Schwabx, C. (2002). Fast deterministic pricing of options on levy driven assets. Technical report, Risk Lab, ETH, Zurich.
Meerschaert, M. M., & Tadjeran, C. (2004). Finite difference approximations for fractional advection–dispersion flow equations. *Journal of Computational and Applied Mathematics, 172*, 65–77.
Meerschaert, M. M., & Tadjeran, C. (2006). Finite difference approximations for two-sided space-fractional partial differential equations. *Applied Numerical Mathematics, 56*, 80–90.
Oldham, K. B., & Spanier, J. (1974). *The fractional calculus: Theory and applications of differentiation and integration to arbitrary order*. Mathematics in science and engineering, V. San Diego, CA: Academic Press.
Sousa, E. (2008). Finite difference approximations for a fractional advection diffusion problem. Technical Report 08-26, Departamento de Matematica, Universidade de Coimbra.
Strauss, A. K. (2006). *Numerical analysis of jump-diffusion models for option pricing*. PhD thesis, Virginia Polytechnic Institute and State University.
Tadjeran, C., Meerschaert, M., & Scheffler, H.-P. (2006). A second-order accurate numerical approximation for the fractional diffusion equation. *Journal of Computational Physics, 213*, 205–213.
Tavella, D., & Randall, C. (2000). *Pricing financial instruments. The finite-difference method. Wiley series in financial engineering*. New York: Wiley.

Wilmott, P. (1998). *Derivatives*. New York: Wiley.
Yoshida, H. (1990). Construction of higher order symplectic integrators. *Physics Letters, 150*, 262–268.
Zhang, X. (1993). Numerical-analysis of American option pricing in a jump-diffusion model. *Mathematics of Operations Research, 22*, 668–690.
Zhang, K., & Wang, S. (2009). A computational scheme for options under jump diffusion processes. *International Journal of Numerical Analysis and Modeling, 6*, 110–123.
Zhou, J. (2006). *Option pricing under generalized tempered stable processes*. PhD thesis, University of Delware.